Utrecht University

Master's Thesis

Holographic Fermions: From Black Branes Towards Cold Atoms

Author:

Pim Borman

Supervisors:

Prof. Dr. Ir. H.T.C. Stoof

V.P.J. Jacobs, MSc

Department of Physics and Astronomy

Institute for Theoretical Physics

August 23, 2014

Abstract

Holographic Fermions: From Black Branes Towards Cold Atoms

by Pim BORMAN

In this thesis we will show how to construct spectral functions from a gravitational model, treating it classically such that no string corrections are involved. The particular model we will study is a black brane in a $(4+1)$-dimensional AdS background. Both the charged and uncharged cases which will be covered, corresponding to the presence and absence of a chemical potential, respectively. The ultimate goal is to accurately describe a cold atom gas using holography. This is still something that is left for the future. We did however find some signatures of non-Fermi liquids and multiple Fermi surfaces.

Contents

Chapter 1

Introduction

In this thesis we study the application of Anti-de Sitter/Conformal Field Theory (AdS/CFT) to condensed matter. The AdS/CFT correspondence was first proposed by Juan Maldacena in 1997 [1]. The claim of AdS/CFT is that in certain cases a gravity theory in the a $(d + 1)$-dimensional space, referred to as the bulk, is equivalent to a conformal field theory on the d-dimensional boundary of that space. Most realizations relate a particular supersymmetric conformal field theory to some kind of superstring theory, the most famous example being the equivalence between type IIB string theory on $\mathrm{AdS}_5 \times \mathrm{S}^5$ and $N = 4$ supersymmetric Yang-Mills theory [2]. The approach taken by Maldacena and his followers is known as the top-down approach and it is very much rooted in string theory.

We will take a different approach, known as the bottom-up approach. It is more phenomenological and it is the easiest way to try and relate a gravity theory to the Green's function of a condensed-matter system. Some excellent reviews of the subject are [3],[4],[5]. The reason why we look at asymptotic AdS spacetimes is that this space has a boundary that looks locally like Minkowski space, where quantum field theories live [6]. We assume that we work in the so-called large-N and large 't Hooft coupling limit, which means that the supergravity partition function can be approximated by a classical Einstein-Hilbert action with additional fields.

In the bottom-up approach we just define a classical gravity action and see what kind of quantum field theory comes out, that is we use a mapping $\mathrm{S_{gravity}} \to \mathrm{S_{qft}}$ to find $\mathrm{S_{qft}}$. This procedure is described in [7],[8] and references therein. The resulting field theory will be a-priori strongly coupled. This strong coupling is what it is all about: in condensed matter there are some major problems with strongly coupled materials such as high-temperature superconductors and other strange metals. Perturbation theory breaks down and one of the ideas is that holography could describe these phenomena by

mapping it onto a weakly coupled theory in a curved background. One of the inherent properties of holography is conformal scale invariance, therefore the condensed-matter system that we will describe must have the same scale invariance. An example of a strongly coupled system are ultracold fermionic atoms at unitarity. This is the reason why we focus on an ultracold atom gas near a Feshbach resonance [9]. At zero temperature and zero chemical potential the correlation length goes to infinity rendering the system scale invariant. Even when the system is not exactly critical, meaning that there is a temperature $T > 0$ and a nonzero density in the form of a chemical potential $\mu > 0$, the duality is still assumed to hold. The phase diagram is shown in figure (1.1).
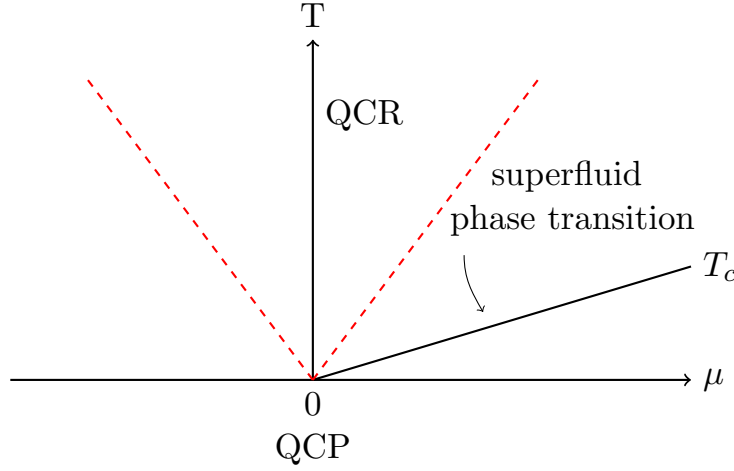

FIGURE 1.1: This is an illustration of the phase diagram. The temperature is denoted by T and the chemical potential by μ. The quantum critical point is at $\mu = T = 0$. It should be possible to detect traces of the quantum phase transition at small enough temperatures in the quantum critical region.

The objective of this thesis is to derive a model that contains the necessary elements of such a system, namely it must contain massive Dirac fermions, that have a nonzero temperature and a chemical potential. Furthermore, since atoms are nonrelativistic, we want to take the nonrelativistic limit of the Green's function. This suppresses the antiparticle degrees of freedom in the model and leaves us with a model that could possible describe ultracold fermionic atoms, like ^{6}Li for example. Concretely, the nonrelativistic dispersion relation will follow from

$$\hbar\omega + \mu = \frac{\hbar^2 \mathbf{k}^2}{2m} + \Sigma(\omega, \mathbf{k}) \ .$$

The self-energy of the system $\Sigma(\omega, \mathbf{k})$ is determined by the coupling of the fermion to the conformal field theory in the bulk.

In addition to the nonrelativistic limit, we will also study the emergence of (multiple) Fermi surfaces in the presence of a chemical potential. These have been found earlier in a 3-dimensional spacetime [10]. These Fermi surfaces will turn out to describe a non-Fermi

liquid instead of a Landau Fermi liquid. This is understandable because Landau Fermi liquids are renormalized to a free Fermi gas with almost no interactions while non-Fermi liquids are believed to be strongly coupled. Examples are high-T_C superconducting cuprates and metals close to a quantum critical point [11].

We are interested in calculating the spectral function $\rho(\omega, \mathbf{k})$ of the field theory on the boundary. It is defined in terms of the retarded Green's function as

$$\rho(\omega, \mathbf{k}) = \frac{1}{\pi} \mathrm{Im} \left(\mathrm{Tr} \left[G_R(\omega, \mathbf{k}) \right] \right) \ .$$

Our approach is different from most bottom-up models because we add a kinetic term to the action by hand. This way the Green's function can be interpreted as a single-particle propagator, obeying the sum rule [7]

$$\int_{-\infty}^{\infty} \mathrm{d}\omega \rho(\omega, \mathbf{k}) = 1 \ .$$

The structure of this thesis is as follows: in Chapter 2 we introduce the gravitational setup leading to the spectral function of a massless chiral fermion. Our particular setup will be an asymptotic Lifshitz space, of which AdS is a special case, with a black brane in it. A black brane is a black hole with a planar geometry. In Chapter 3 we expand this to a massive Dirac fermion. Of this system we will study the CPT symmetries. In Chapter 4 we add a chemical potential by charging the black brane. Finally in Chapter 5 we look at the nonrelativistic limit and investigate some signatures of multiple Fermi surfaces.

Chapter 2

The Chiral Fermion

In this chapter the spectral function of a chiral fermion will be derived. We start with the bulk theory, by first finding the gravitational setup that feeds the right metric and then couple this metric to the fermions in the fermion action. We neglect the backreaction of the fermions on the metric.

2.1 The Bulk Description

2.1.1 The Background Metric

First we review how anti-de Sitter spacetime is obtained from Einsteins equations, and after that we will generalize this to a Lifshitz spacetime.

The starting point is the Einstein-Hilbert action,

$$S_{EH} = \frac{1}{16\pi G_{d+1}} \int \mathrm{d}^{d+1}x \sqrt{-g}(R - 2\Lambda) \ , \tag{2.1}$$

where d is the number of spacetime dimensions on the boundary and G_{d+1} is Newtons constant in $d+1$ dimensions. Later on we will focus on $d = 4$, but we describe the holographic setup for general d. The covariant measure is $\mathrm{d}^{d+1}x\sqrt{-g}$, where $g = \det(g_{\mu\nu})$, with $g_{\mu\nu}$ the components of the metric. The stress-energy tensor is defined by

$$T_{\mu\nu} = -\frac{2}{\sqrt{-g}}\frac{\delta S_M}{\delta g^{\mu\nu}} \ . \tag{2.2}$$

The matter action S_M is given by

$$S_M = \int \mathrm{d}^{d+1}x \sqrt{-g}\mathcal{L}_M \ , \tag{2.3}$$

with $\mathcal{L}_M$ the Lagrangian density of the matter fields, specified later. Varying the background action $S_{bg} = S_{EH} + S_M$ with respect to $g^{\mu\nu}$ gives us the well-known Einsteins equations,

$$R_{\mu\nu} - \frac{1}{2}Rg_{\mu\nu} + \frac{1}{2}\Lambda g_{\mu\nu} = 8\pi G_{d+1}T_{\mu\nu} \ . \tag{2.4}$$

The sign of Λ, the matter fields in $\mathcal{L}_M$ and the imposed symmetries specify the metric. A good illustration of this approach is the Reissner-Nordström black hole in $d + 1 = 4$ dimensions. It is a spherically symmetric solution in Minkowski space, i.e. $\Lambda = 0$, and $\mathcal{L}_M = -\frac{1}{4}F_{\mu\nu}F^{\mu\nu}$ only contains the electric field. $F_{\mu\nu}$ is called the electromagnetic field tensor and is defined in terms of the electromagnetic potential by $F_{\mu\nu} = \partial_\mu A_\nu - \partial_\nu A_\mu$. The Einstein's equations read

$$R_{\mu\nu} - \frac{1}{2}Rg_{\mu\nu} + \frac{1}{2}\Lambda g_{\mu\nu} = 8\pi G_{d+1}\left(F_{\mu\alpha}F^\alpha_\rho - \frac{1}{4}g_{\mu\nu}F_{\alpha\beta}F^{\alpha\beta}\right) \ . \tag{2.5}$$

Since we only consider an electric field in the r-direction we can put $F_{rt} = Q/r^2$ and $A_i = 0$. Here Q is the charge of the black hole. The solution reads:

$$ds^2_{RN} = -V^2(r)dt^2 + \frac{1}{V^2(r)}dr^2 + r^2d\Omega^2_2 \ , \ \ V^2(r) = 1 - \frac{2G_4M}{r} + \frac{G_4Q^2}{r^2} \ . \tag{2.6}$$

Another example is pure AdS spacetime in $d + 1$ dimensions, corresponding to the case where $\Lambda < 0$ and $\mathcal{L}_M = 0$. The metric reads

$$ds^2_{AdS} = -\frac{r^2}{\ell^2}dt^2 + \frac{\ell^2}{r^2}dr^2 + \frac{r^2}{\ell^2}dx^2_{d-1} \ , \tag{2.7}$$

where ℓ is the AdS-radius. When we transform to another coordinate frame where $z^2 = \ell^4/r^2$, the metric takes the form

$$ds^2_{AdS} = \frac{\ell^2}{z^2}\left(-dt^2 + dz^2 + dx^2_{d-1}\right) \ . \tag{2.8}$$

Here we see clearly that the space consists of slices at constant r (z) and that with increasing r (decreasing z) the slices grow with a factor $\frac{r^2}{\ell^2}$. This is graphically depicted in figure (2.1). A special feature of AdS spacetime that is not present in Minkowski or dS spacetime is that light can reach the $r = \infty$ limit in finite time. This means that there is a notion of a boundary of AdS spacetime which has the topology of Minkowski spacetime. This is important since the field theory we will be considering lives on this boundary. The line element ds^2_{AdS} is invariant under the isotropic scalings

$$t \to \lambda t, \ \ x_i \to \lambda x_i, \ \ r \to \lambda^{-1}r \ . \tag{2.9}$$

These scalings will correspond to relativistic scalings on the boundary. It can sometimes be useful to consider more general scalings, called Lifshitz scalings, since condensed-matter systems are often nonrelativistic. These anisotropic scalings read

$$t \to \lambda t^z, \quad x_i \to \lambda x_i, \quad r \to \lambda^{-1} r . \tag{2.10}$$

In this thesis mainly the $z = 1$ case is discussed, but for clarity and future work, we will describe the setup for general z. The metric of pure Lifshitz space time reads

$$ds^2_{AdS} = -\frac{r^{2z}}{\ell^{2z}} dt^2 + \frac{\ell^2}{r^2} dr^2 + \frac{r^2}{\ell^2} dx^2_{d-1} . \tag{2.11}$$

What we want to find is a black brane solution that is an asymptotically Lifshitz spacetime instead of a Minkowski spacetime, and that has a planar symmetry. First we will consider the uncharged black brane and later, in chapter 4, we will consider the charged case. This means we want to find a setup of which the following metric is the solution:

$$ds^2 = -\frac{V^2(r)r^{2z}}{\ell^{2z}} dt^2 + \frac{\ell^2}{V^2(r)r^2} dr^2 + \frac{r^2}{\ell^2} dx^2_{d-1} . \tag{2.12}$$

Here the function $V(r)$ is called the emblackening factor that should be zero at the black brane horizon and equal to one on the boundary. From now on we will set $\ell = 1$. It can always be put back by analyzing the dimensions, something that we will do in section 4.1. It turns out that the following setup solves the problem [12]:

$$\mathcal{L}_M = -\frac{1}{32\pi G_{d+1}} \left(\partial_\mu \phi \partial^\mu \phi + e^{\lambda_1 \phi} F_{1\mu\nu} F_1^{\mu\nu} \right) , \quad \Lambda = -(d+z-1)(d+z-2) . \tag{2.13}$$

The matter field ϕ is a dilaton and $F_{1\mu\nu}$ is antisymmetric, just as the electromagnetic tensor. It should be stressed that these fields are only used to give the right metric $g_{\mu\nu}$. They will not couple to the fermion and will not have any direct influence on the spectral functions. Possible divergences on the boundary are therefore not problematic. This means that F_1 should not be interpreted as the electromagnetic field strength tensor, it just has the same form. The solutions of the equations of motion of these matter fields are

$$e^{\lambda_1 \phi} = 2(z-1)(d+z-1)\frac{1}{f^2} r^{2(1-d)}, \quad F_{1rt} = f r^{(d+z-2)} , \tag{2.14}$$

where $\lambda_1 = -\sqrt{\frac{2(d-1)}{z-1}}$ and f is a free constant. Einstein's equations now give the metric (2.12) with emblackening factor

$$V^2(r) = 1 - \left(\frac{r_h}{r} \right)^{(d+z-1)} . \tag{2.15}$$

Indeed we see that $V(r_h) = 0$ and $V(r \to \infty) \to 1$.

Like a black hole, a black brane has a Hawking temperature that is given by

$$T = \frac{1}{4\pi}\frac{\partial \left(V^2\right)}{\partial r}|_{r=r_h}r_h^{z+1} \; . \tag{2.16}$$

This expression is obtained from Wick-rotating to imaginary time such that the time-coordinate is periodic and then demanding the absence of a conical singularity.[3] For our metric the temperature reduces to

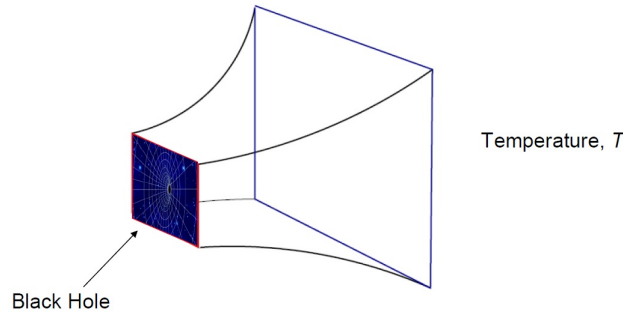$$T = \frac{d+z-1}{4\pi}r_h^z \; . \tag{2.17}$$

FIGURE 2.1: The black brane radiates such that the Hawking temperature on the horizon is equal to the temperature on the boundary. Adapted from a presentation by David Tong.

Because Lifshitz spacetime has a boundary, this boundary can be in thermal equilibrium with the bulk. This way the Hawking temperature of the black brane will be the same as the temperature of the system on the boundary. This is illustrated in figure (2.1).

It should be noted that the fields ϕ and F_1 could in principle diverge on the boundary, the metric however does not. The fermions we will be considering are only coupled to the metric and we ignore their influence on the metric, the backreaction. Therefore we do not need to worry about these divergences. They will not influence the boundary theory of the fermions. Furthermore, in the $z = 1$ case the fields decouple such that $\mathcal{L}_M = 0$ and we end up with Einstein's equations in vacuum.

2.1.2 The Dirac Equation in the Bulk

Now that we obtained the background metric we will be working with, namely, asymptotically Lifshitz spacetime with a planar Schwarzschild black brane, it is time to add fermions to the bulk. The fermions are described by the Dirac action that is $(d+1)$-dimensional and in a curved background. To describe this we need $(d+1)$-dimensional gamma matrices and the spin connection to make the Lagrangian covariant. First we

will introduce the gamma matrices in a flat background and after that generalize it to a curved background.

The Dirac equation reads

$$(\slashed{\partial} - M)\Psi = 0 \ , \tag{2.18}$$

where $\slashed{\partial} = \Gamma^{\underline{a}}\partial_{\underline{a}}$. We use the underline $\underline{a}$ to indicate that the coordinate is in a flat background, furthermore $\Gamma^{\underline{a}}$ denote the gamma matrices in the $(d+1)$-dimensional bulk whereas $\gamma^{\underline{a}}$ denote the gamma matrices on the d-dimensional boundary. From the context it should be clear which indices we sum over when using the Einstein summation convention; for example in $\Gamma^{\underline{a}}\partial_{\underline{a}}$ we have $\underline{a} \in \{\underline{r}, \underline{t}, \underline{i}\}$ whereas for $\gamma^{\underline{a}}\partial_{\underline{a}}$ we have $\underline{a} \in \{\underline{t}, \underline{i}\}$. The matrices $\gamma^{\underline{a}}$ form a d-dimensional representation of the Clifford algebra, which means they obey the anticommutation relation

$$\{\gamma^{\underline{a}}, \gamma^{\underline{b}}\} = 2\eta^{ab}\mathbb{1}_N \ , \tag{2.19}$$

and have dimension $N = 2^{\lfloor \frac{d}{2} \rfloor}$. This also means that the spinor Ψ has $2^{\lfloor \frac{d}{2} \rfloor}$ components.

The Γ's obey the same anticommutation relation and have dimension $N = 2^{\lfloor \frac{d+1}{2} \rfloor}$. This $(d+1)$-dimensional representation is constructed in the following way. First we have to distinguish between the cases where d is even or odd. It turns out that every even-dimensional representation is reducible, which means that we can define an analog of the usual γ^5, denoted by $\gamma^{\underline{d+1}}$, that splits the Dirac spinor into two chiral components. This is not possible for an odd-dimensional representation.

When d is odd, the dimension of the Γ's is twice the dimension of the γ's. In the chiral representation we have explicitly:

$$\Gamma^{\underline{r}} = \begin{pmatrix} \mathbb{1}_{\lfloor \frac{d}{2} \rfloor} & 0 \\ 0 & -\mathbb{1}_{\lfloor \frac{d}{2} \rfloor} \end{pmatrix}, \ \Gamma^{\underline{t}} = \begin{pmatrix} \gamma^{\underline{0}} & 0 \\ 0 & \gamma^{\underline{0}} \end{pmatrix}, \ \Gamma^{\underline{i}} = \begin{pmatrix} \gamma^{\underline{i}} & 0 \\ 0 & \gamma^{\underline{i}} \end{pmatrix}, \ \Psi = \begin{pmatrix} \Psi_+ \\ \Psi_- \end{pmatrix} \ . \tag{2.20}$$

Here the Dirac spinor Ψ in the bulk is split in its two chiral components. When restricted to the boundary these chiral components become Dirac spinors. This procedure is followed by McGreevy et al. in [4] because they look at $d = 2 + 1$.

We however are interested in the case where d is even. Then the dimension of the Γ's is the same as the dimension of the γ's. Explicitly they read:

$$\Gamma^{\underline{r}} = \gamma^{\underline{d+1}}, \quad \Gamma^{\underline{t}} = \gamma^{\underline{0}}, \quad \Gamma^{\underline{i}} = \gamma^{\underline{i}}, \quad \Psi \ . \tag{2.21}$$

Here Ψ is a Dirac spinor and it cannot be split into chiral components in the bulk. Therefore on the boundary it is possible to do this:

$$\Psi_R = \begin{pmatrix} \Psi_+ \\ 0 \end{pmatrix} = \frac{1}{2}\left(\mathbb{1}_{2^{d/2}} + \gamma^{\underline{d+1}}\right)\Psi, \quad \Psi_L = \begin{pmatrix} 0 \\ \Psi_- \end{pmatrix} = \frac{1}{2}\left(\mathbb{1}_{2^{d/2}} - \gamma^{\underline{d+1}}\right)\Psi . \quad (2.22)$$

For reference we state the explicit expressions of the gamma matrices in the Weyl representation in $d = 4$:

$$\gamma^{\underline{d+1}} = \begin{pmatrix} \mathbb{1}_2 & 0 \\ 0 & -\mathbb{1}_2 \end{pmatrix}, \quad \gamma^{\underline{t}} = \begin{pmatrix} 0 & -\mathbb{1}_2 \\ \mathbb{1}_2 & 0 \end{pmatrix}, \quad \gamma^{\underline{i}} = \begin{pmatrix} 0 & \sigma^i \\ \sigma^i & 0 \end{pmatrix}, \quad (2.23)$$

Where σ^i are the Pauli matrices. We will describe the holographic procedure for even d in the next section, and after that use the above expressions to get concrete results for the $d = 4$ case. For odd d the procedure is a bit different since the Dirac fermion on the boundary cannot be split into chiral components.

Now that we have found the arbitrary dimensional representations of the gamma matrices in flat spacetime, it is time to generalize it to curved spacetime. This means setting $\eta^{\underline{ab}} \to g^{\mu\nu}$. The greek indices indicate we work in a curved spacetime. The gamma matrices change accordingly: $\gamma^{\underline{a}} \to \gamma^\mu$ and $\Gamma^{\underline{a}} \to \Gamma^\mu$ such that the anticommutation relation (2.19) changes to be

$$\{\gamma^\mu, \gamma^\nu\} = 2g^{\mu\nu}\mathbb{1}_N . \quad (2.24)$$

These changes are accommodated by so-called vielbeins $e^\mu_{\underline{a}}$. These are objects that define a locally flat coordinate frame at every spacetime point. They are defined as

$$\eta_{\underline{ab}} = e^\mu_{\underline{a}}e^\nu_{\underline{b}}g_{\mu\nu} . \quad (2.25)$$

We need them since we want to work with the flat gamma matrices instead of the curved ones. The vielbeins relate them to each other by $\gamma^\mu = e^\mu_{\underline{a}}\gamma^{\underline{a}}$. Contractions such as the one in the Dirac equation (2.18) transform as

$$\Gamma^{\underline{a}}\partial_{\underline{a}} \to \Gamma^\mu\partial_\mu = e^\mu_{\underline{a}}\Gamma^{\underline{a}}\partial_\mu . \quad (2.26)$$

To make the Dirac Lagrangian covariant we also need to introduce a covariant derivative. For a tensor field this would just be the Levi-Civita connection. However, for a spinor field we have to add an extra term that acts on flat spacetime indices $\underline{a}, \underline{b}$ etcetera, and on the spinor indices of Ψ. This term is called the spin connection and is denoted by $\omega_{\mu\underline{ab}}$. On a generalized tensor that has both curved and flat spacetime indices, such as

the vielbein e^a_μ, the covariant derivative acts as

$$D_\mu e^a_\nu = \partial_\mu e^a_\nu + \omega_\mu{}^a{}_{\underline{b}} e^b_\nu + \Gamma^\sigma_{\mu\nu} e^a_\sigma \ . \tag{2.27}$$

The metric compatibility condition $D_\mu g_{\nu\rho} = 0$ of the Levi-Civita connection is equivalent to $D_\mu e^a_\nu = 0$. This gives us the following expression for $\omega_{\mu\underline{ab}}$:

$$\omega_{\mu\underline{ab}} = e_{\nu\underline{a}} \partial_\mu e^\nu_{\underline{b}} + e_{\nu\underline{a}} e^\sigma_{\underline{b}} \Gamma^\nu_{\sigma\mu} \ . \tag{2.28}$$

The Christoffel symbols can in principle be expressed in terms of the vielbeins via equation (2.25).

To see how the covariant derivative acts on a spinor Ψ we remember that under an infinitesimal Lorentz transformation, Ψ transforms as

$$\Psi \to \left(1 + \frac{1}{4} \Omega_{\underline{ab}}(x) S^{\underline{ab}} \right) \Psi \ . \tag{2.29}$$

Here, $S^{\underline{ab}} = \frac{1}{2}[\Gamma^{\underline{a}}, \Gamma^{\underline{b}}]$, and $\Omega_{\underline{ab}}(x)$ depends on x since the Lorentz transformations are only defined locally through the vielbeins. This is why $\partial_\mu \Psi$ does not transform covariantly. The covariant derivative becomes

$$D_\mu \Psi = \left(\partial_\mu + \frac{1}{4} \omega_{\mu\underline{ab}} S^{\underline{ab}} \right) \Psi \ . \tag{2.30}$$

More details about the spin connection can be found in [13]. The covariant Dirac equation becomes:

$$\left(\Gamma^{\underline{a}} e^\mu_{\underline{a}} D_\mu - M \right) \Psi = 0 \ . \tag{2.31}$$

We will now give explicit expressions for the vielbeins of the black brane metric (2.12):

$$e^r_{\underline{r}} = rV, \quad e^t_{\underline{t}} = \frac{1}{r^z V}, \quad e^i_{\underline{i}} = \frac{1}{r} \ . \tag{2.32}$$

The covariant derivative takes the form

$$D_r = \partial_r, \quad D_t = \partial_t - \frac{1}{2} rV \partial_r(r^z V) \Gamma^{\underline{t}} \Gamma^{\underline{r}}, \quad D_i = \partial_i + \frac{1}{2} rV \Gamma^{\underline{i}} \Gamma^{\underline{r}} \ . \tag{2.33}$$

In this background we will construct the fermion action in the bulk.

2.1.3 Building the Fermion Action in the Bulk

With all the ingredients of the previous section we can now write down the action for a Dirac fermion in the bulk:

$$S_D[\Psi] = i g_f \int \mathrm{d}^{d+1}x \sqrt{-g}\, \bar{\Psi} \left(\frac{1}{2}\overrightarrow{\slashed{D}} - \frac{1}{2}\overleftarrow{\slashed{D}} - M \right) \Psi \ . \tag{2.34}$$

Here g_f is a coupling constant and the i is put in front by convention. The r coordinate ranges between the horizon of the black brane r_h and the boundary r_0 that we will later take to infinity. The variation of the action results in the equation of motion plus boundary terms at r_h and r_0 due to partial integration. The induced metric $h_{\mu\nu}$ on a constant r-slice is defined by $\sqrt{-g} = \sqrt{-h}\sqrt{g_{rr}}$. And the Γ^r matrix can be used to split Ψ into its chiral components on the boundary, see equation (2.22). Using these facts we can write the variation as

$$\delta S_D = \ \text{E.O.M.} \ + i\frac{g_f}{2} \int \mathrm{d}^d x \sqrt{-h} \left(\bar{\Psi}_L \delta\Psi_R + \delta\bar{\Psi}_R \Psi_L - \bar{\Psi}_R \delta\Psi_L - \delta\bar{\Psi}_L \Psi_R \right) |_{r=r_h}^{r=r_0} \ . \tag{2.35}$$

Because $\sqrt{-h}|_{r=r_h} = 0$, the boundary terms at the horizon vanish. To make the boundary terms at the boundary vanish we need to add a counterterm. Note that because the Dirac equation is first order, we can impose a Dirichlet boundary condition at r_0; either $\delta\Psi_R = 0$ or $\delta\Psi_L = 0$. We cannot impose both since the Dirac equation relates both components to each other. We add the following term to the action:

$$S_\partial = \pm i\frac{g_f}{2} \int_{r=r_0} \mathrm{d}^d x \sqrt{-h} \left(\bar{\Psi}_L \Psi_R + \bar{\Psi}_R \Psi_L \right) \ , \tag{2.36}$$

where we choose the $+$ sign if $\delta\Psi_R = 0$ and the $-$ sign if $\delta\Psi_L = 0$. Mixed boundary conditions are also possible, but these violate Lorentz symmetry on the boundary [14]. We now have

$$\delta \left(S_D + S_\partial \right) = 0 \ . \tag{2.37}$$

From now on we will consider the case where $\delta\Psi_R = 0$ on the boundary. As long as the variation is zero we can add more terms, in particular we can add a kinetic term to the UV boundary:

$$S_{UV} = iZ \int_{r=r_0} \mathrm{d}^d x \sqrt{-h}\sqrt{g_{rr}}\, \bar{\Psi}_R \slashed{D} \Psi_R \ , \tag{2.38}$$

where Z is an arbitrary constant. We will see later that this kinetic term describes the free dynamics of the fermion on the boundary while the other part of the action describes

the interactions. This term has to be added to make the spectral functions obey the ARPES sum-rule [7]. We stress again that Ψ_R describes a chiral fermion on the boundary. Would we have chosen d to be odd, it would describe a Dirac fermion. Furthermore, the fermion on the boundary is massless, the bulk mass M becomes just a parameter in the interaction. The three terms above constitute the full action of the chiral fermion we are describing,

$$S_{full} = S_D + S_\partial + S_{UV} \ . \tag{2.39}$$

In the next section we restrict the fermions to the boundary and obtain a Green's function for them.

2.2 The Boundary Description

Before we do this, there is another point we have to pay attention to; we want to find the retarded Green's function, which in general is complex. It turns out that when we keep both terms in S_∂ the propagator is real. The solution is to drop one of the terms. The following expression corresponds to the retarded Green's function:

$$S_\partial = i g_f \int_{r=r_0} \mathrm{d}^d x \sqrt{-h} \left(\bar{\Psi}_R \Psi_L \right), \quad \delta \Psi_R = 0 \ , \tag{2.40}$$

$$S_\partial = -i g_f \int_{r=r_0} \mathrm{d}^d x \sqrt{-h} \left(\bar{\Psi}_L \Psi_R \right), \quad \delta \Psi_L = 0 \ . \tag{2.41}$$

An extra factor of 2 is included for consistency.

2.2.1 The Boundary Action of the Chiral Fermion

As stated before, the Dirac equation relates the chiral components $\Psi_R = \begin{pmatrix} \Psi_+ \\ 0 \end{pmatrix}$ and $\Psi_L = \begin{pmatrix} 0 \\ \Psi_- \end{pmatrix}$ to each other in the following way:

$$\Psi_- = -i\xi \Psi_+ \ . \tag{2.42}$$

In $d = 4$, ξ is a 2 x 2 matrix that can be determined by solving the Dirac equation. This will be explained in the next subsection. The above expression is used to integrate out Ψ_L on the boundary when we choose $\delta \Psi_R = 0$ and Ψ_R on the boundary when we choose

$\delta\Psi_L = 0$. The Fourier-transformed spinors on each r-slice are defined as

$$\Psi_\pm(r,x) = \int \frac{\mathrm{d}^d p}{(2\pi)^d} \Psi_\pm(r,k) e^{ip_\mu x^\mu} \ . \tag{2.43}$$

In the $\delta\Psi_R = 0$ case we end up with the following effective action $S_{full}[\Psi_+]$ for the chiral fermion Ψ_+ on the boundary:

$$S_{full}[\Psi_+] = -\int_{r=r_0} \frac{\mathrm{d}^d p}{(2\pi)^d} \sqrt{-h}\sqrt{g_{rr}} \Psi_+^\dagger \left[g_f \sqrt{g^{rr}} \xi(\omega, \mathbf{k}) - Z\sigma^{\underline{a}} e^\mu_{\underline{a}} p_\mu \right] \Psi_+ \ , \tag{2.44}$$

Here we used the fact that the spin-connection vanishes on the boundary as can be show explicitly by using the expressions in equation (2.33). Furthermore $\sigma^{\underline{a}} = (\mathbb{1}_2, \vec{\sigma})$ with $\vec{\sigma}$ the Pauli matrices. Note that the the summation indices μ and $\underline{a}$ are only over $\{t, i\}$. When we now do a rescaling of the fields by

$$\Psi_+ \to \Psi_+ Z^{-1/2} r_0^{(2-d)/2} V^{1/2}(r_0) \ , \tag{2.45}$$

the action takes the form

$$S_{full}[\Psi_+] = -\int \frac{\mathrm{d}^d k}{(2\pi)^d} \Psi_+^\dagger \left[\omega - V(r_0) r_0^{z-1} \vec{\sigma} \cdot \mathbf{k} + \frac{g_f}{Z} r_0^{z+1} V^2(r_0) \xi \right] \Psi_+ \ . \tag{2.46}$$

The effective action for Ψ_+ now contains a self-energy term related to the solution of the Dirac equation in the bulk. The term between the square brackets is the inverse Green's function we are interested in:

$$G_R^{-1}(\omega, \mathbf{k}) = -\left(\omega - V(r_0) r_0^{z-1} \vec{\sigma} \cdot \mathbf{k} + \frac{g_f}{Z} r_0^{z+1} V^2(r_0) \xi \right) \ . \tag{2.47}$$

This is the Green's function of the elementary chiral field Ψ_+. The challenge is to find an expression for the self-energy ξ. Before we turn to this, it is useful to see what happens when we take the limit $r_0 \to \infty$.

As $r_0 \to \infty$ the emblackening factor $V(r_0) \to 1$. The second term in (2.47) is divergent for $z > 1$. After renormalization it becomes [7] :

$$-\frac{1}{\lambda} \vec{\sigma} \cdot \mathbf{k} |\mathbf{k}|^{z-1} \ . \tag{2.48}$$

Here λ is a renormalization parameter which we choose to be $\lambda = 1$. For the third term we use the fact that for large r_0, $\xi \sim r_0^{-2M}$, which means that $r_0^{2M}\xi \to$ constant. To make the whole term finite on the boundary we must take a double scaling limit

$$r_0 \to \infty, \qquad g_f \to 0, \qquad g \equiv \frac{g_f}{Z} r_0^{1+z-2M} \to \text{constant} \ . \tag{2.49}$$

The third term in equation (2.47) can then be written as

$$\Sigma(\omega, \mathbf{k}) \equiv -g \lim_{r_0 \to \infty} r_0^{2M} \xi(r_0, \omega, \mathbf{k}) \ . \tag{2.50}$$

Using these renormalizations the Green's function becomes finite on the boundary and takes the form

$$G_R^{-1}(\omega, \mathbf{k}) = -\left[\omega - \vec{\sigma} \cdot \mathbf{k} |\mathbf{k}|^{z-1} - \Sigma(\omega, \mathbf{k})\right] \ . \tag{2.51}$$

All we need to do now is invert this expression and solve the Dirac equation to find $\xi(r, \omega, \mathbf{k})$ and hence $\Sigma(\omega, \mathbf{k})$.

2.2.2   Solving the Dirac Equation for ξ

Solving the equation for ξ is the main point of this thesis. Especially in the presence of a chemical potential this turns out to be quite difficult and we have to use numerical techniques to find solutions. We will use $d = 4$ dimensions such that Ψ is a 4-component spinor and ξ is a 2 x 2 matrix. When we choose $\mathbf{k} = (0, 0, k_3)$ the matrix ξ will be diagonal because the 4 x 4 matrices that appear in the Dirac equation are build from the diagonal 2 x 2 blocks $\mathbb{1}_2$ and σ^3:

$$\Psi_- = -i \begin{pmatrix} \xi_+ & 0 \\ 0 & \xi_- \end{pmatrix} \Psi_+ \ , \tag{2.52}$$

where $\xi_+(r, \omega, k_3)$ and $\xi_-(r, \omega, k_3)$ are the functions we have to determine. Because of rotational invariance it is possible to rotate the solution back to general $\mathbf{k}$ such that for large r_0, $\xi \propto \sigma^\mu k_\mu$. The components of $\Psi = \begin{pmatrix} \Psi_+ \\ \Psi_- \end{pmatrix}$ are given by $\Psi_\pm = \begin{pmatrix} u_\pm \\ d_\pm \end{pmatrix}$. In terms of these we have

$$\xi_+ = i \frac{u_-}{u_+}, \qquad \xi_- = i \frac{d_-}{d_+} \ . \tag{2.53}$$

To solve the Dirac equation we assume a plane wave ansatz on a constant r-slice

$$\Psi(x) = e^{i k_\mu x^\mu} \Psi(r) \ . \tag{2.54}$$

For the covariant derivative $\not{D} = \Gamma^{\underline{a}} e_{\underline{a}}^{\mu} D_{\mu}$ we use the expressions in equations (2.32) and (2.33). The Dirac equation can now be expressed as

$$
\begin{aligned}
0 &= \left(\not{D} - M \right) \Psi(x) \\
&= \left(\not{D} - M \right) e^{i k_{\mu} x^{\mu}} \Psi(r) \\
&= \left[\Gamma^{\underline{r}} rV \partial_r + \Gamma^{\underline{t}} (r^z V)^{-1} \left(\partial_t - \frac{1}{2} rV \partial_r (r^z V) \Gamma^{\underline{t}} \Gamma^{\underline{r}} \right) \right. \\
&\qquad\qquad \left. + \Gamma^{\underline{i}} \frac{1}{r} \left(\partial_i + \frac{1}{2} rV \Gamma^{\underline{i}} \Gamma^{\underline{r}} \right) - M \mathbb{1}_4 \right] e^{ik \cdot x} \Psi(r) \quad (2.55) \\
&= \left[\Gamma^{\underline{r}} rV \partial_r + \frac{i}{r} \left(\Gamma^{\underline{i}} k_i - \Gamma^{\underline{t}} \frac{\omega}{r^{z-1}V} \right) + \frac{1}{2} \Gamma^{\underline{r}} \partial_r (r^z V) r^{z-1} \right. \\
&\qquad\qquad \left. + \frac{1}{2} \Gamma^{\underline{r}} V (d-1) - M \mathbb{1}_4 \right] e^{ik \cdot x} \Psi(r) \, ,
\end{aligned}
$$

Where in the third line a sum over i is understood. Define

$$
\tilde{k} \equiv (-\tilde{\omega}, \mathbf{k}), \quad \tilde{\omega} \equiv -\frac{\omega}{r^{z-1}V} \, , \tag{2.56}
$$

$$
\Gamma \cdot \tilde{k} = \Gamma^{\underline{i}} k_i - \Gamma^{\underline{t}} \frac{\omega}{r^{z-1}V}, \quad p_z(r) = r^{z-1} \partial_r (r^z V) + (d-1)V \, . \tag{2.57}
$$

Furthermore let Φ be defined by

$$
\Psi(r) = e^{-\frac{1}{2} \int^r d\tilde{r} \frac{p_z(\tilde{r})}{\tilde{r} V(\tilde{r})}} \Phi(r) \, . \tag{2.58}
$$

The Dirac equation then simplifies to

$$
\left(\Gamma^{\underline{r}} rV \partial_r + \frac{i}{r} \Gamma \cdot \tilde{k} - M \mathbb{1}_4 \right) \Phi(r) = 0 \, , \tag{2.59}
$$

$$
\Rightarrow \begin{pmatrix} r(rV\partial_r - M) & 0 \\ 0 & -r(rV\partial_r + M) \end{pmatrix} \begin{pmatrix} \phi_+ \\ \phi_- \end{pmatrix} + i\Gamma \cdot \tilde{k} \begin{pmatrix} \phi_+ \\ \phi_- \end{pmatrix} = 0 \, . \tag{2.60}
$$

This gives us the following equations for the components of $\phi_{\pm} = \begin{pmatrix} \tilde{u}_{\pm} \\ \tilde{d}_{\pm} \end{pmatrix}$:

$$
\mathcal{A}(M)\tilde{u}_+ = i(\tilde{\omega} - k_3)\tilde{u}_-, \quad \mathcal{A}(-M)\tilde{u}_- = i(\tilde{\omega} + k_3)\tilde{u}_+ \, , \tag{2.61}
$$

$$
\mathcal{A}(M)\tilde{d}_+ = i(\tilde{\omega} + k_3)\tilde{d}_-, \quad \mathcal{A}(-M)\tilde{d}_- = i(\tilde{\omega} - k_3)\tilde{d}_+ \, . \tag{2.62}
$$

Here $\mathcal{A}(M) = r(rV - M)$. The ratio of any of the components of Φ is equal to the ratio of the components of Ψ. Using this and equation (2.53) we obtain a differential equation

for $\xi_+(r, \omega, k_3)$

$$r^2 V \partial_r \xi_+ = i r^2 V \partial_r \frac{u_-}{u_+} \tag{2.63}$$

$$= \frac{i}{u_+} \left[\mathcal{A}(-M) u_- - M r u_- - \frac{u_-}{u_+} (\mathcal{A}(M) u_+ + r M u_+) \right] \tag{2.64}$$

$$= -(\tilde{\omega} + k_3) - (\tilde{\omega} - k_3) \xi_+^2 - 2 M r \xi_+ . \tag{2.65}$$

The same can be done for ξ_- and the result can be written as

$$r^2 V \partial_r \xi_\pm + 2 M r \xi_\pm = -\tilde{\omega} \mp k_3 + (-\tilde{\omega} \pm k_3) \xi_\pm^2 , \tag{2.66}$$

where we note that $\tilde{\omega}$ depends on r through $\tilde{\omega} = \frac{-\omega}{r^{z-1} V}$. This is a first order nonlinear differential equation in r, which means we need to specify one boundary condition. We choose infalling boundary conditions corresponding with particles falling into the black brane. It follows that we need [15]

$$\xi_\pm(r_h, \omega, k_3) = i \qquad \text{for} \quad \omega \neq 0 . \tag{2.67}$$

Equation (2.66) has some symmetries we can exploit. When $k_3 \to -k_3$:

$$\xi_\pm(r, \omega, -k_3) = \xi_\mp(r, \omega, k_3) , \tag{2.68}$$

when $(\omega, k_3) \to (-\omega, k_3)$:

$$\xi_\pm(r, -\omega, -k_3) = -\xi_\pm^*(r, \omega, k_3) , \tag{2.69}$$

when $M \to -M$:

$$\xi_\pm(r, -M, \omega, k_3) = -\xi_\pm^{-1}(r, M, \omega, -k_3) . \tag{2.70}$$

These symmetries can be used to simplify the (numerical) calculations. We will for example only solve the differential equation for ξ_+ and use equation (2.68) to get ξ_-. It turns out to be very difficult to find analytic solutions for ξ, which is why we will mainly solve the differential equation numerically. Some more details on how to do this are given in section 5.2 in the context of a charged black brane. Only in some special cases we can

find an analytic solution. For example when $T = 0$ and $z = 1$ we find for $r \gg 1$ [16]

$$\xi = \begin{pmatrix} \xi_+ & 0 \\ 0 & \xi_- \end{pmatrix} \tag{2.71}$$

$$= (2r)^{-2M} \frac{\Gamma(\frac{1}{2} - M)}{\Gamma(\frac{1}{2} + M)} e^{-i\pi(M + \frac{1}{2})} \sqrt{\omega^2 - k_3^2}^{2M-1} (-\omega \mathbb{1}_2 + \sigma^3 k_3) . \tag{2.72}$$

This expression can be rotated back for general **k**.

2.3 The Spectral Function

To calculate the spectral function we expand the self-energy $\Sigma(\omega, \mathbf{k})$ as $\Sigma = -\Sigma_0 \mathbb{1}_2 + \Sigma_3 \sigma_3$. This can later be rotated to obtain

$$\Sigma = \Sigma_\mu \sigma^\mu, \quad \sigma^\mu = (\mathbb{1}_2, \sigma^i) . \tag{2.73}$$

With the help of symmetry (2.68) the matrix ξ can be written as

$$\xi(\omega, k_3) = \begin{pmatrix} \xi_+(\omega, k_3) & 0 \\ 0 & \xi_+(\omega, -k_3) \end{pmatrix} = \begin{pmatrix} \xi_+^s(\omega, k_3) + \xi_+^a(\omega, k_3) & 0 \\ 0 & \xi_+^s(\omega, k_3) - \xi_+^a(\omega, k_3) \end{pmatrix} , \tag{2.74}$$

where the symmetric part is $\xi_+^s(\omega, k_3) = \frac{1}{2}[\xi_+(\omega, k)) + \xi_+(\omega, -k_3)]$ and the antisymmetric part is $\xi_+^a(\omega, k_3) = \frac{1}{2}[\xi_+(\omega, k)) - \xi_+(\omega, -k_3)]$. This way we can identify

$$\Sigma_0(\omega, k_3) = -g \lim_{r_0 \to \infty} r_0^{2M} [-\xi_+^s(r_0, \omega, k_3)] , \tag{2.75}$$

$$\Sigma_3(\omega, k_3) = -g \lim_{r_0 \to \infty} r_0^{2M} [\xi_+^a(r_0, \omega, k_3)] . \tag{2.76}$$

The inverse Green's function (2.47) now has the form

$$G_R^{-1}(\omega, \mathbf{k}) = - \left[\omega \mathbb{1}_2 - \vec{\sigma} \cdot \mathbf{k} |\mathbf{k}|^{z-1} - \Sigma_\mu \sigma^\mu \right] . \tag{2.77}$$

With the help of the identity $a_\mu a_\nu \sigma^\mu \bar{\sigma}^\nu = a_\mu a^\mu \mathbb{1}_2$, we find

$$G_R(\omega, \mathbf{k}) = - \frac{(\omega - \Sigma_0) \mathbb{1}_2 + (|\mathbf{k}|^{z-1} k_i + \Sigma_i) \sigma^i}{(\omega - \Sigma_0)^2 - (|\mathbf{k}|^{z-1} k_i + \Sigma_i)^2} . \tag{2.78}$$

The spectral function becomes

$$\rho(\omega, \mathbf{k}) = \frac{1}{\pi}\text{Im}\left(\text{Tr}\left[G_R(\omega, \mathbf{k})\right]\right) \tag{2.79}$$

$$= -\frac{1}{\pi}\text{Im}\left[\frac{\omega - \Sigma_0}{(\omega - \Sigma_0)^2 - (|\mathbf{k}|^{z-1}k_i + \Sigma_i)^2}\right] \ .$$

The spectral function is plotted in figure (2.3) for some parameter values. The linear behavior at large ω and k when $z = 1$ signifies relativistic scaling. This is only the spectral function of the massless chiral fermion Ψ_+. It has been shown [7] that the spectral function satisfies the sum rule

$$\int_{-\infty}^{\infty} \mathrm{d}\omega \rho(\omega, \mathbf{k}) = 1 \tag{2.80}$$

for $-z/2 < M < z/2$. For this reason we usually take $-1/2 < M < 1/2$. Figure (2.2) shows an illustration of the holographic description. In the next chapter we will extend this description to a massive Dirac fermion since in condensed matter that is what we are interested in.

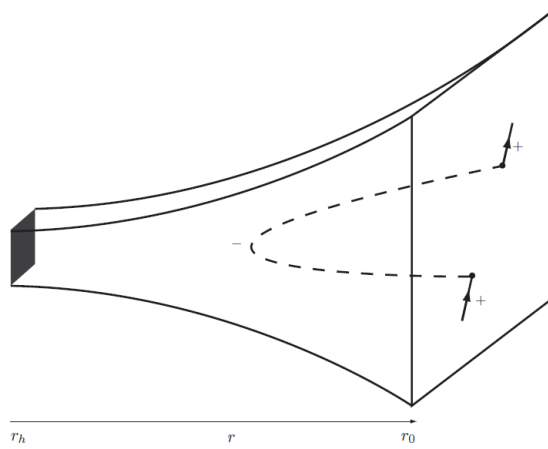FIGURE 2.2: Illustration of the holographic description. Equation (2.78) describes the chiral (+) single-particle propagator on the boundary. The fermions interact with each other which is described by Ψ_- traveling into the bulk, feeling classically the gravitational effects by coupling to the conformal field theory, and coming out again, forming the self-energy of the single fermions. The figure is extracted from [16].

(A) $M = 1/4$, $z = 1$

(B) $M = -1/4$, $z = 1$

(C) $M = 1/4$, $z = 2$

(D) $M = -1/4$, $z = 2$
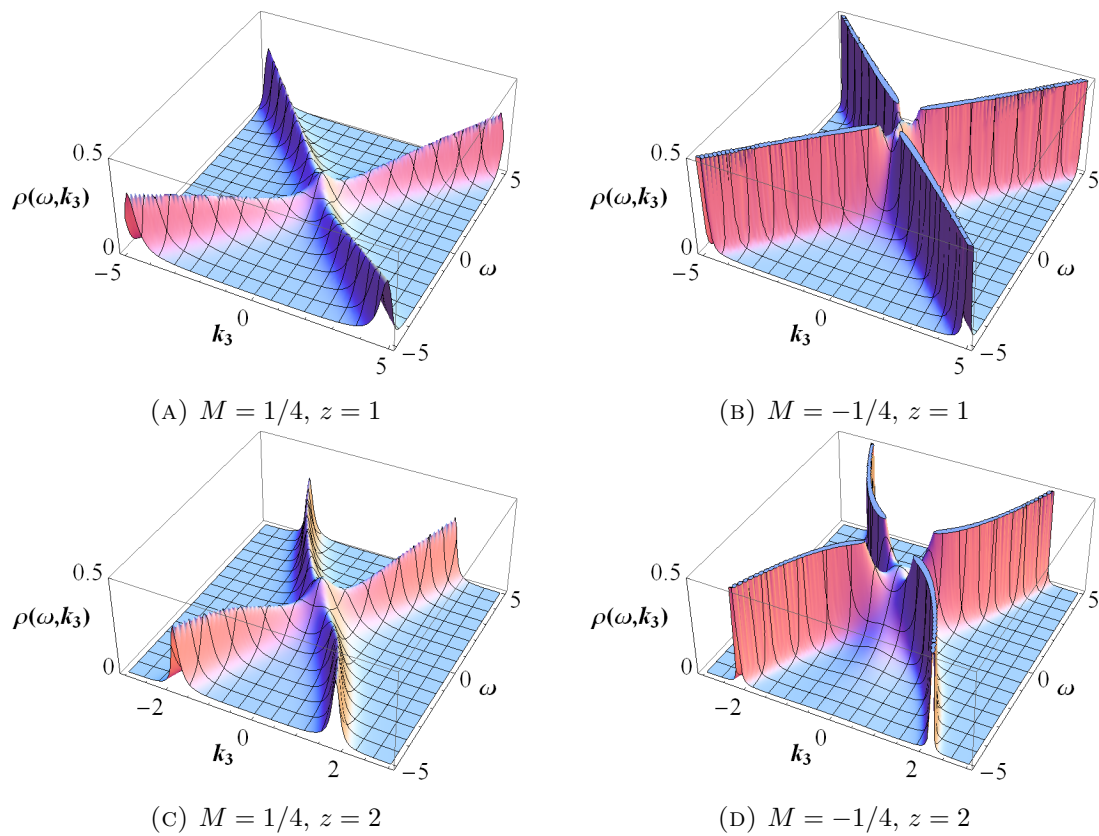
FIGURE 2.3: Plots of the spectral function (2.79) of the chiral fermion Ψ_+ for different M and z. The relativistic behaviour for $z = 1$ is clearly visible at large ω, k_3. For negative M the spectral function is sharply peaked while for positive M it is more broad. For all plots we used $T = 1$ and $g = 1$. The qualitative behaviour is independent of g.

Chapter 3

The Dirac Fermion

In this chapter the Dirac fermion is introduced. In the first section the massless case is described and in the second section the fermion is given a mass. After that the Green's function is split into its eigenvalues describing a spin-1/2 particle or antiparticle. In the last section we investigate the how the system behaves under C, P and T transformations.

3.1 The Massless Dirac Fermion

3.1.1 Derivation of the Effective Action

The way to obtain a Dirac fermion on the boundary is to add another fermion to the bulk. This will result in two chiral fermions on the boundary with opposite chirality that can be combined in a single Dirac spinor. This procedure will be explained below. We add a second fermion Ψ_2 to the bulk action (2.39) as follows

$$S_D[\Psi_2] = i g_f \int \mathrm{d}^{d+1}x \sqrt{-g}\,\bar{\Psi}_2 \left(\frac{1}{2}\overrightarrow{\slashed{D}} - \frac{1}{2}\overleftarrow{\slashed{D}} - M_2 \right) \Psi_2 \ , \tag{3.1}$$

$$S_\partial[\Psi_2] = -i g_f \int_{r=r_0} \mathrm{d}^d x \sqrt{-h}\left(\bar{\Psi}_{2R}\Psi_{2L} \right) \ , \tag{3.2}$$

$$S_{UV}[\Psi_2] = i Z \int_{r=r_0} \mathrm{d}^d x \sqrt{-h}\sqrt{g_{rr}}\,\bar{\Psi}_{2L}\slashed{D}\Psi_{2L} \ . \tag{3.3}$$

For the second fermion we choose the boundary condition $\delta\Psi_{2L} = 0$ and *not* $\delta\Psi_{2R} = 0$ like before. This means we must take the $-$ sign in equation (3.2) to cancel the boundary terms. To obtain the retarded Green's function we dropped one term in $S_\partial[\Psi_2]$, as explained before in equation (2.41).

In $d = 4$ the Dirac equation relates $\Psi_{2,+}$ and $\Psi_{2,-}$ by the 2 x 2 matrix ξ_2

$$\Psi_{2,+} = i\xi_+^{-1}\Psi_{2,-} \ . \tag{3.4}$$

Note that this is slightly different from the definition of ξ_1. Using this relation $\Psi_{2,+}$ can be integrated out. In momentum space we obtain the following effective action of the second chiral fermion on the boundary

$$S_{full}[\Psi_{2,-}] = \int_{r=r_0} \frac{\mathrm{d}^4 p}{(2\pi)^4} \sqrt{-h}\sqrt{g_{rr}}\Psi_{2,-}^\dagger \left[g_{f,2}\sqrt{g^{rr}}\xi_2^{-1} - Z\bar{\sigma}^{\underline{a}}e_{\underline{a}}^\mu p_\mu \right] \Psi_{2,-} \ . \tag{3.5}$$

This should be added to the effective action of the first chiral fermion, given in equation (2.44). The Dirac fermion Ψ we will be describing is defined by

$$\Psi = \begin{pmatrix} \Psi_{1,+} \\ \Psi_{2,-} \end{pmatrix} \ . \tag{3.6}$$

The combined effective action is given by

$$S_{full}[\Psi] = \int_{r=r_0} \frac{\mathrm{d}^4 p}{(2\pi)^4} \sqrt{-h}\sqrt{g_{rr}}\bar{\Psi} \left[\sqrt{g^{rr}}\xi - Ze_{\underline{a}}^\mu\gamma^\mu p_\mu \right] \Psi \ , \tag{3.7}$$

where we used

$$\xi \equiv \begin{pmatrix} 0 & g_{f,2}\xi_2^{-1} \\ g_{f,1}\xi_1 & 0 \end{pmatrix} \quad \text{and} \quad \gamma^\mu = \begin{pmatrix} 0 & \bar{\sigma}^\mu \\ \sigma^\mu & 0 \end{pmatrix} \ . \tag{3.8}$$

After rescaling Ψ the same way as $\Psi_{1,+}$ in equation (2.45) we obtain

$$S_{full}[\Psi] = \int_{r=r_0} \frac{\mathrm{d}^4 k}{(2\pi)^4} \bar{\Psi} \left[\gamma^0\omega - V(r_0)r_0^{z-1}\gamma^i k_i + \frac{1}{Z}r_0^{z+1}V^2(r_0)\xi \right] \Psi \ . \tag{3.9}$$

We now take two double scaling limits and do it in such a way that we obtain one coupling constant g in front of the self-energy

$$r_0 \to \infty \qquad g \equiv \frac{g_{f,1}}{Z}r_0^{1+z-2M_1} = \frac{g_{f,2}}{Z}r_0^{1+z+2M_2} \to \text{ constant} \ . \tag{3.10}$$

$$g_{f,1}, \ g_{f,2} \to 0$$

The action now reads

$$S_{full}[\Psi] = \int_{r=r_0} \frac{\mathrm{d}^4 k}{(2\pi)^4} \bar{\Psi} \left[\gamma^0\omega - \gamma^i k_i |\mathbf{k}|^{z-1} - \Sigma(\omega, \mathbf{k}) \right] \Psi \ , \tag{3.11}$$

where we renormalized the second term and defined the self-energy as

$$\Sigma(\omega, \mathbf{k}) \equiv -g \begin{pmatrix} 0 & \lim_{r_0 \to \infty} r_0^{-2M_2} \xi_2^{-1} \\ \lim_{r_0 \to \infty} r_0^{2M_1} \xi_1 & 0 \end{pmatrix} . \tag{3.12}$$

The inverse Green's function can be identified as

$$G_R^{-1}(\omega, \mathbf{k}) = \gamma^0 \left(\gamma^0 \omega - \gamma^i k_i |\mathbf{k}|^{z-1} - \Sigma(\omega, \mathbf{k}) \right) . \tag{3.13}$$

We will now expand the matrix ξ in gamma matrices. Because we chose the mass of the second fermion to be equal to $-M_2$ we can use equation (2.70) to write $\xi_2^{-1}(r, M_2, \omega, \mathbf{k}) = -\xi_2(r, -M_2, \omega, -\mathbf{k})$. When restricting to the k_3 direction and using symmetry (2.68) we obtain

$$\xi = \begin{pmatrix} 0 & -\xi_2(r, -M_2, \omega, -k_3) \\ \xi_1(r, M_1, \omega, k_3) & 0 \end{pmatrix} \tag{3.14}$$

$$= \begin{pmatrix} 0 & 0 & -\xi_{2+}(\omega, -k_3) & 0 \\ 0 & 0 & 0 & -\xi_{2+}(\omega, k_3) \\ \xi_{1+}(\omega, k_3) & 0 & 0 & 0 \\ 0 & \xi_{1+}(\omega, -k_3) 0 & 0 & 0 \end{pmatrix}, \tag{3.15}$$

where the dependence on M_1, M_2, r is implied. The symmetric parts ξ_{1s}, ξ_{2s} in k_3 and antisymmetric parts ξ_{1a}, ξ_{2a} in k_3 are defined as in equation (2.74). In terms of these we get

$$\xi(\omega, k_3) = \begin{pmatrix} 0 & \xi_{2S}\bar{\sigma}^t + \xi_{2A}\bar{\sigma}^3 \\ \xi_{1S}\sigma^t + \xi_{1A}\sigma^3 & 0 \end{pmatrix} \tag{3.16}$$

$$= \begin{pmatrix} 0 & \xi_{2\mu}\bar{\sigma}^\mu \\ \xi_{1\mu}\sigma^\mu & 0 \end{pmatrix}, \tag{3.17}$$

where $\xi_{i,0} \equiv \xi_{iS}$ and $\xi_{i,3} \equiv \xi_{iA}$. Expanded in gamma matrices this gives

$$\xi(\omega, k_3) = \frac{1}{2}(\xi_{1\mu} + \xi_{2\mu})\gamma^\mu + \frac{1}{2}(\xi_{1\mu} - \xi_{2\mu})\gamma^\mu \gamma^5 . \tag{3.18}$$

The corresponding self-energy terms are defined by

$$\Sigma_{i\mu} = -g \lim_{r_0 \to \infty} r^{\pm 2M_i} \xi_{i\mu}(\mathbf{k}, \omega) . \tag{3.19}$$

The inverse Green's function now takes the form

$$G_R^{-1}(\omega, \mathbf{k}) = \gamma^0 \left[\gamma^0 \omega - \gamma^i k_i |\mathbf{k}|^{z-1} - \frac{1}{2} \left(\Sigma_{1\mu} + \Sigma_{2\mu} \right) \gamma^\mu - \frac{1}{2} \left(\Sigma_{1\mu} - \Sigma_{2\mu} \right) \gamma^\mu \gamma^5 \right] . \tag{3.20}$$

3.1.2 The Spectral Function of a Massless Dirac Fermion

The differential equation for ξ_{2+} is the same as for ξ_{1+} as given in equation (2.66) but with a different sign in front of M_2. Therefore if $M_1 = -M_2$ the self-energy terms are equal,

$$M_1 = -M_2 \quad \to \quad \Sigma_{1\mu} = \Sigma_{2\mu} \ , \tag{3.21}$$

and the γ^5 term cancels. In general however this term is present and we will see later that it breaks for example parity. Using the following formula we can invert equation (3.20)

$$\left[\gamma^0 \left(a\gamma^0 - b_i\gamma^i + c\gamma^0\gamma^5 - d_i\gamma^i\gamma^5 \right) \right]^{-1} = \tag{3.22}$$
$$\frac{1}{AB} \{ \ [a(A+B) + c(B-A)]\gamma^0 - [b_i(A+B) + d_i(B-A)]\gamma^i$$
$$- [c(A+B) - a(B-A)]\gamma^0\gamma^5 + [d_i(A+B) - b_i(B-A)]\gamma^i\gamma^5 \ \}\gamma^0 \ ,$$

$$\text{with} \quad A = (a+c)^2 - (b_i - d_i)^2 \quad \text{and} \quad B = (a-c)^2 - (b_i - d_i)^2 \ .$$

As a result the Green's function can be written as

$$G_R(\mathbf{k}, \omega) = -\frac{1}{2} \left[\frac{\omega - \Sigma_{1_0}}{A} + \frac{\omega - \Sigma_{2_0}}{B} \right] \mathbb{1}_4 \tag{3.23}$$
$$- \frac{1}{2} \left[\frac{\omega - \Sigma_{1_0}}{A} - \frac{\omega - \Sigma_{2_0}}{B} \right] \gamma^5$$
$$- \frac{1}{2} \left[\frac{k_i|\mathbf{k}|^{z-1} + \Sigma_{1_i}}{A} + \frac{k_i|\mathbf{k}|^{z-1} + \Sigma_{2_i}}{B} \right] \gamma^i\gamma^0$$
$$- \frac{1}{2} \left[\frac{k_i|\mathbf{k}|^{z-1} + \Sigma_{1_i}}{A} - \frac{k_i|\mathbf{k}|^{z-1} + \Sigma_{2_i}}{B} \right] \gamma^i\gamma^0\gamma^5 \ ,$$

with

$$A = -(k_i|\mathbf{k}|^{z-1} + \Sigma_{1_i})^2 + (\omega - \Sigma_{1_0})^2 \ ,$$
$$B = -(k_i|\mathbf{k}|^{z-1} + \Sigma_{2_i})^2 + (\omega - \Sigma_{2_0})^2 \ .$$

This can be written a bit more transparently in 2 x 2 matrix form

$$G_R(\mathbf{k}, \omega) = -\begin{pmatrix} \frac{(\omega - \Sigma_{1,0})\mathbb{1}_2 + (k_i|\mathbf{k}|^{z-1} + \Sigma_{1,i})\sigma^i}{(\omega - \Sigma_{1,0})^2 - (k_i|\mathbf{k}|^{z-1} + \Sigma_{1,i})^2} & 0 \\ 0 & \frac{(\omega - \Sigma_{2,0})\mathbb{1}_2 - (k_i|\mathbf{k}|^{z-1} + \Sigma_{2,i})\sigma^i}{(\omega - \Sigma_{2,0})^2 - (k_i|\mathbf{k}|^{z-1} + \Sigma_{2,i})^2} \end{pmatrix} \ . \tag{3.24}$$

Due to the absence of a boundary mass term there is no mixing between the chiral components. The spectral function is just the sum of the two, normalized with an

additional factor of $\frac{1}{2}$,

$$\rho(\omega, k_3) = -\frac{1}{2\pi} \left[\frac{\omega - \Sigma_{1,0}}{(\omega - \Sigma_{1,0})^2 - (k_3|k_3|^{z-1} + \Sigma_{1,3})^2} \right. $$
$$\left. + \frac{\omega - \Sigma_{2,0}}{(\omega - \Sigma_{2,0})^2 - (k_3|k_3|^{z-1} + \Sigma_{2,3})^2} \right] . \quad (3.25)$$

In figure (3.1) the spectral function of Ψ is plotted. These plots look very much the same as those in figure (2.3). This is because we take the trace over all components and there are no off-diagonal terms in $G_R(\omega, \mathbf{k})$ that mix the chiral components. In figure (3.2) the spectral functions of the four individual eigenvalues of $G_R(\omega, \mathbf{k})$ are plotted.

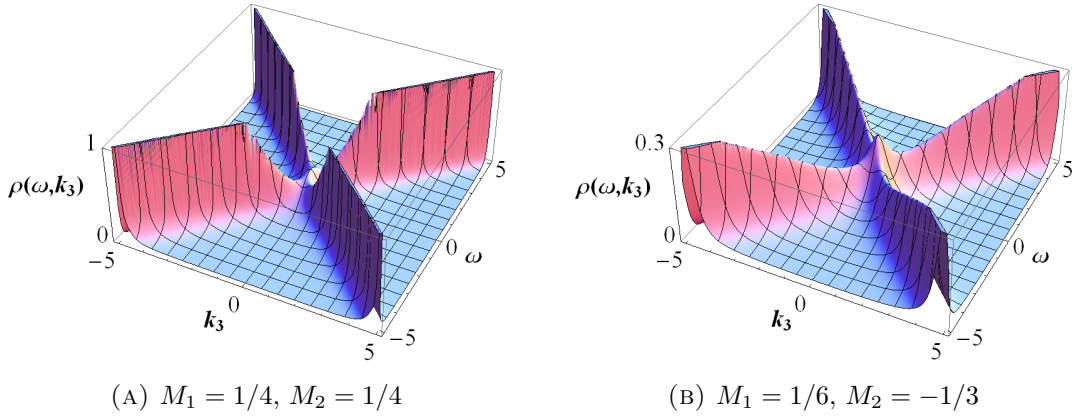(A) $M_1 = 1/4$, $M_2 = 1/4$ (B) $M_1 = 1/6$, $M_2 = -1/3$

FIGURE 3.1: Plots of the spectral function (3.25) of the Dirac fermion Ψ for different M_1 and M_2. The following parameters are used: $z = 1$, $g = 1$ and $T = 1$. The heights are taken differently just for esthetic reasons. The plots can still be compared qualitatively.

(A) first component

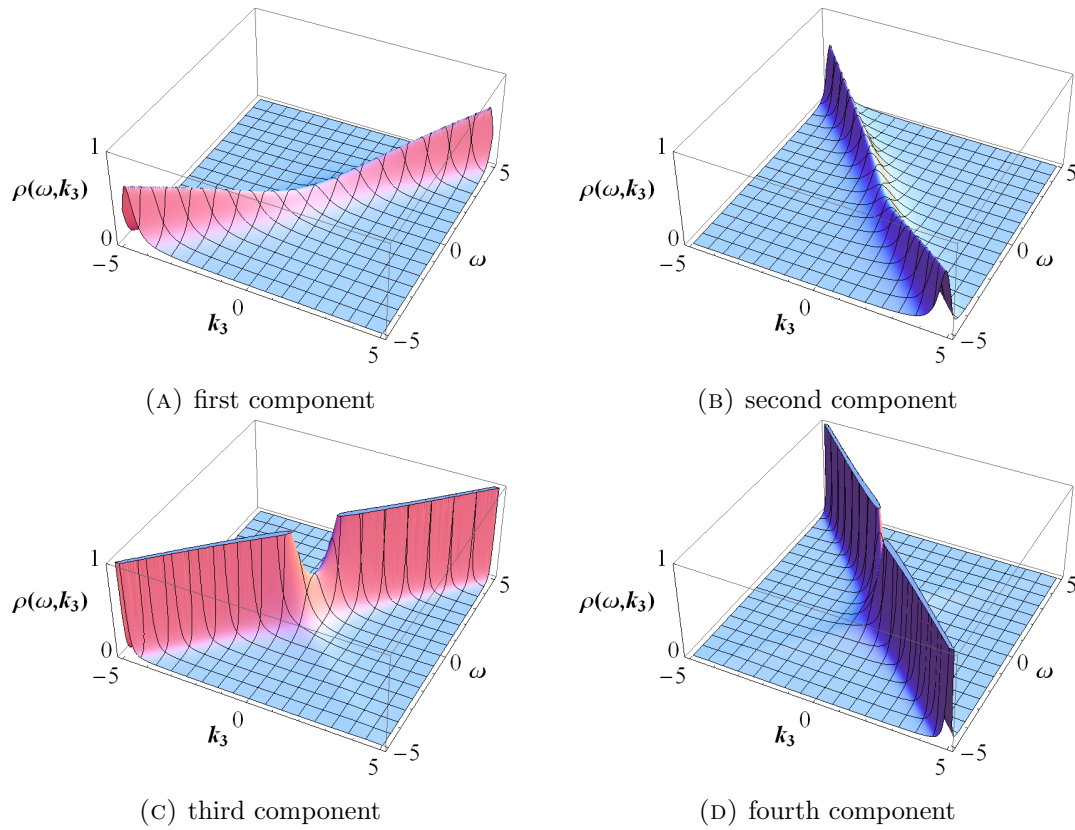(B) second component

(C) third component

(D) fourth component

FIGURE 3.2: Plotted are the spectral functions of the four individual eigenvalues of $G_R(\omega, k_3)$. The following parameters are used: $M_1 = M_2 = 1/4$, $z = 1$, $g = 1$ and $T = 1$. The normalized sum of figures (a)-(d) results in figure (3.1a).

3.2 The Massive Dirac Fermion

Now it is time to give the boundary fermion a mass m. This is done by introducing yet another term to the bulk action,

$$S_m[\Psi] = -iZ \int_{r=r_0} \mathrm{d}^4x \sqrt{-h}\, \bar{\Psi} m \Psi \ . \tag{3.26}$$

It can be added because the variation is zero

$$\delta S_m \sim \Psi^\dagger_{2,-}\delta\Psi_{1+} + \delta(\Psi^\dagger_{2,-})\Psi_{1,+} - \Psi^\dagger_{1,+}\delta\Psi_{2,-} - \delta(\Psi^\dagger_{1,+})\Psi_{2,-} \tag{3.27}$$

$$= 0 \ . \tag{3.28}$$

After rescaling Ψ as described before and m as $m \to mr^{-z}$ the $r_0 \to \infty$ limit gives

$$S_m[\Psi] = -i \int \frac{\mathrm{d}^4p}{(2\pi)^4}\Psi^\dagger\gamma^0 m\Psi \ . \tag{3.29}$$

The inverse Green's function reads

$$G_R^{-1}(\omega,\mathbf{k}) = \gamma^0 \left[\gamma^0\omega - \gamma^i k_i |\mathbf{k}|^{z-1} - \frac{1}{2}\left(\Sigma_{1\mu} + \Sigma_{2\mu}\right)\gamma^\mu - \frac{1}{2}\left(\Sigma_{1\mu} - \Sigma_{2\mu}\right)\gamma^\mu\gamma^5 - im\mathbb{1}_4 \right] \ . \tag{3.30}$$

Because γ^0 is off-diagonal, the mass term mixes the chiral components. The following formula is used to invert this expression. Here we only consider the k_3 direction.

$$G_R(\omega,\mathbf{k}) = \left[\gamma^0(a\gamma^0 - b_3\gamma^3 + c\gamma^0\gamma^5 - d_3\gamma^3\gamma^5 - im\mathbb{1}_4) \right]^{-1} \tag{3.31}$$

$$= \frac{1}{AB}\left[\{a(-a^2 + c^2 + b_3^2 + d_3^2 + m^2) - 2cb_3d_3\}\mathbb{1}_4 \right.$$

$$+ \{c(a^2 - c^2 + b_3^2 + d_3^2 - m^2) - 2ab_3d_3\}\gamma^5$$

$$+ \{b_3(-a^2 - c^2 + b_3^2 - d_3^2 + m^2) + 2acd_3\}\gamma^3\gamma^0$$

$$+ \{d_3(-a^2 - c^2 - b_3^2 + d_3^2 - m^2) + 2acb_3\}\gamma^3\gamma^0\gamma^5$$

$$+ \{-im(-a^2 + c^2 + b_3^2 - d_3^2 + m^2)\}\gamma^0$$

$$\left. + \{-im(2cb_3 - 2ad_3)\}\gamma^3\gamma^5 \right] \ ,$$

$$\text{where} \quad A = (a - d_3)^2 - (b_3 - c)^2 - m^2 \quad \text{and} \quad B = (a + d_3)^2 - (b_3 + c)^2 - m^2$$

The components are defined as follows

$$a = \omega - \frac{1}{2}(\Sigma_{1,0} + \Sigma_{2,0}) \ , \qquad\qquad c = -\frac{1}{2}(\Sigma_{1,0} - \Sigma_{2,0}) \ ,$$

$$b_3 = \frac{1}{2}(\Sigma_{1,3} + \Sigma_{2,3}) + |k|^{z-1}k_3 \ , \qquad\qquad d_3 = \frac{1}{2}(\Sigma_{1,3} - \Sigma_{2,3}) \ .$$

The corresponding spectral function $\rho(\omega, k_3) = \frac{1}{4\pi} \text{Im} \left(\text{Tr} \left[G_R(\omega, k_3) \right] \right)$ is plotted in figure (3.3). We see that the mass term m opens a gap between the upper, conductance band and the lower, valence band. This motivates the interpretation of m as a mass of the Dirac fermion. The spectral function still looks highly symmetric, but this is because we sum over the spin up and down components when taking the trace. In the next section we will look at the eigenvalues.
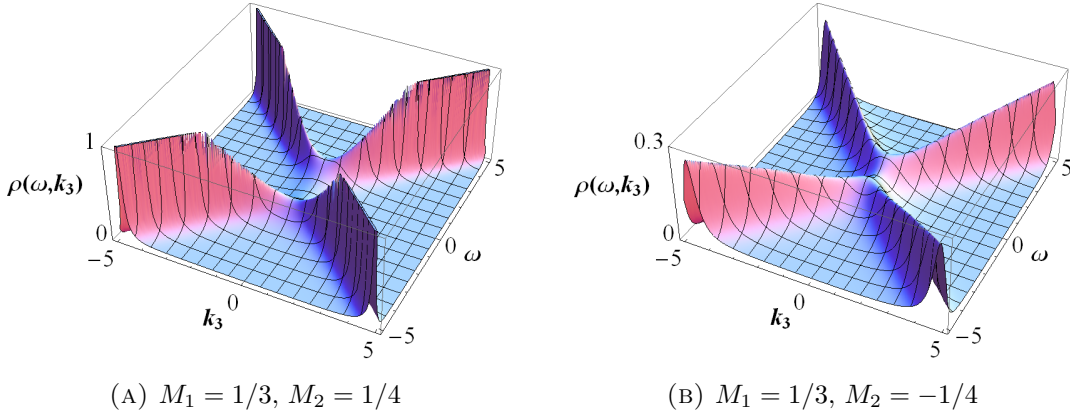

(A) $M_1 = 1/3$, $M_2 = 1/4$ (B) $M_1 = 1/3$, $M_2 = -1/4$

FIGURE 3.3: Plots of the spectral function (3.31) of the Dirac fermion Ψ for different M_1 and M_2. Clearly there is a gap between the upper and lower band. This is caused by the mass term m. The following parameters are used: $z = 1$, $m = 2$, $g = 1$ and $T = 1$.

3.3 Eigenvalues of the Green's Function

The eigenvalues and corresponding eigenvectors of the Green's function are given in tables (3.1) and (3.2). It can be checked that when $m = 0$ the eigenvalues are equal to the diagonal components of equation (3.24). In the $M_1 = -M_2$ case the chiral components are equal to each other and the γ^5 terms vanish. This means that the eigenvalues become degenerate: $e_1 = e_3$ and $e_2 = e_4$.

eigenvalue	eigenvector
$e_1 = -\frac{a - d_3 + \sqrt{(b_3 - c)^2 + m^2}}{A}$	$v_1 = \left(i(b_3 - c + \sqrt{(b_3 - c)^2 + m^2}),\ 0\ ,\ m\ ,\ 0\ \right)$
$e_2 = -\frac{a - d_3 - \sqrt{(b_3 - c)^2 + m^2}}{A}$	$v_2 = \left(i(b_3 - c - \sqrt{(b_3 - c)^2 + m^2}),\ 0\ ,\ m\ ,\ 0\ \right)$
$e_3 = -\frac{a + d_3 + \sqrt{(b_3 + c)^2 + m^2}}{B}$	$v_3 = \left(0,\ i(-b_3 - c + \sqrt{(b_3 + c)^2 + m^2})\ ,\ 0\ ,\ m\ \right)$
$e_4 = -\frac{a + d_3 - \sqrt{(b_3 + c)^2 + m^2}}{B}$	$v_4 = \left(0,\ i(-b_3 - c - \sqrt{(b_3 + c)^2 + m^2})\ ,\ 0\ ,\ m\ \right)$

TABLE 3.1: The eigenvalues and eigenvectors of the Green's function (3.31) are shown.

The spin is determined by acting with the spin operator S_3 on an eigenvector. The spectral functions of the eigenvalues are shown in figure (3.4). These plots show clearly

eigenvalue	spin	particle
e_1	up	particle
e_2	up	anti-particle
e_3	down	particle
e_4	down	anti-particle

TABLE 3.2: The spin state and particle/antiparticle nature of the four eigenvalues of the Green's function(3.31) are shown. Spin up and down correspond with eigenvalues $+1$ and -1 of S^3. It is a particle when it describes the conductance band and it is an antiparticle when it describes the valence band.

that parity is broken when $M_1 \neq -M_2$. In the next section we investigate more thoroughly the CPT symmetries.

(A) first component

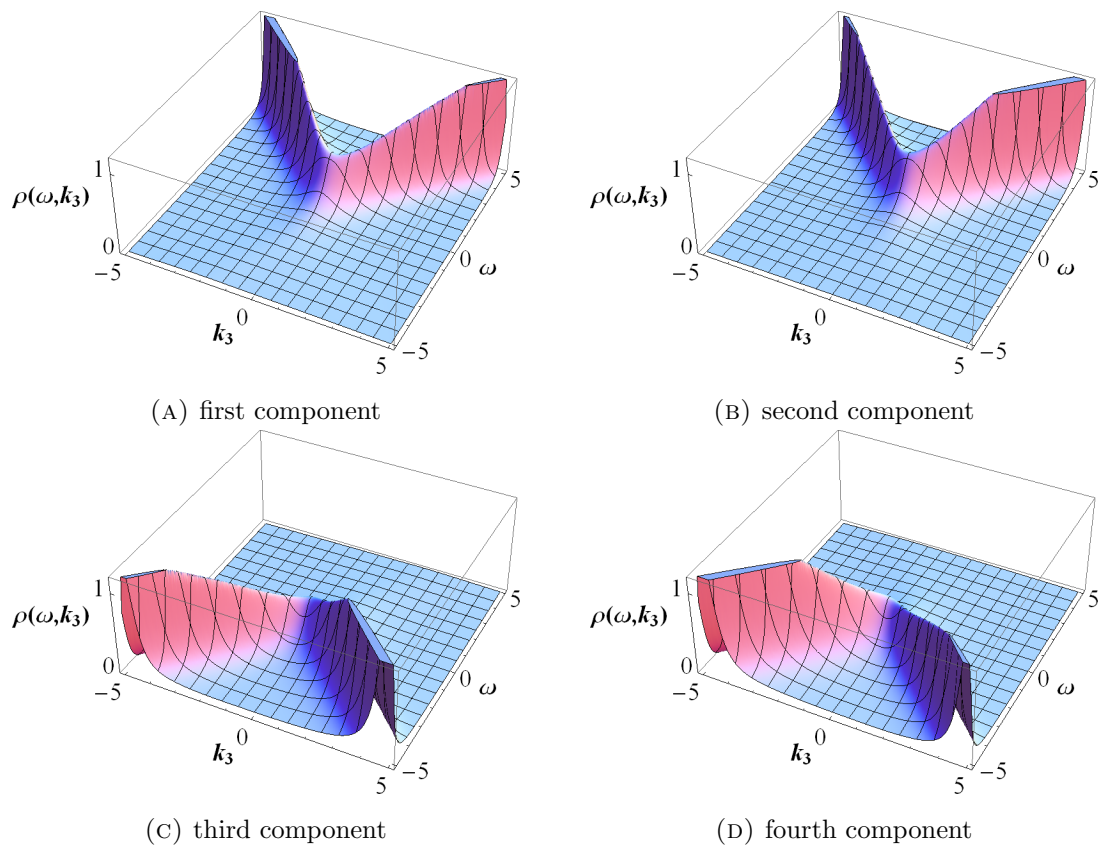(B) second component

(C) third component

(D) fourth component

FIGURE 3.4: Plotted are the spectral functions of the four individual eigenvalues of $G_R(\omega, k_3)$. Parity is seen to be broken because the transformation $k_3 \to -k_3$ is not a symmetry of the system anymore. See the paragraph about parity in section 3.4 for calculational details. The following parameters are used: $M_1 = 1/3$, $M_2 = -1/4$, $m = 2$, $z = 1$, $g = 1$ and $T = 1$. The normalized sum of figures (a)-(d) results in figure (3.3b).

3.4   C P T Symmetries

The single particle Hamiltonian H of the system is related to the inverse Green's function by $G_R^{-1}(\omega, \mathbf{k}) = H - \omega \mathbb{1}_4$. It reads

$$H = \gamma^0 [\alpha \gamma^0 - b_3 \gamma^3 + c \gamma^0 \gamma^5 - d_3 \gamma^3 \gamma^5 - im \mathbb{1}_4] \ , \tag{3.32}$$

where $\alpha = a - \omega$. For reference we state in table (3.3) how the coefficients of the Hamiltonian transform under k_3 and ω inversion.

$k_3 \to -k_3$	$\omega \to -\omega$
$b_3 \to -b_3$	$b_3 \to b_3^*$
$d_3 \to -d_3$	$d_3 \to d_3^*$
$a, \alpha \to a, \alpha$	$a, \alpha \to -a^*, -\alpha^*$
$c \to c$	$c \to -c^*$

TABLE 3.3: Symmetries of the coefficients of the Hamiltonian H.

In this section we will study **C**harge conjugation, **P**arity, and **T**ime reversal symmetries in the $M_1 = -M_2$ and $M_1 \neq -M_2$ cases. To understand how these symmetries act on spinors we start with the free Dirac field, whose Hamiltonian is invariant under all these symmetries. This procedure is described in [17]. Below we will state the results in our representation and signature. The free one particle Dirac Hamiltonian in position space is

$$H_D = \gamma^0 (-i \gamma^i \partial_i + im) \ . \tag{3.33}$$

First look at the positive frequency solutions of the Dirac equation. The wavefunction has the form $\Psi(x, t) = u(p) e^{-ip \cdot x}$ where $p_\mu = (-E, p_1, p_2, p_3)$ such that $p^2 = -m^2$ and

$$(\partial\!\!\!/ - m) u(p) e^{-ip \cdot x} = 0 \ . \tag{3.34}$$

It follows that $u(p) e^{-ip \cdot x}$ is an eigenstate of H_D with eigenvalue $E_{\mathbf{k}} > 0$. We have

$$u^s(p) = \begin{pmatrix} \sqrt{p \cdot \bar{\sigma}} \ \xi^s \\ \sqrt{-p \cdot \sigma} \ i \xi^s \end{pmatrix} \ , \tag{3.35}$$

where ξ^s is a basis of the two component spin vector with two degrees of freedom $s = 1, 2$ and normalized by $\xi^{s\dagger} \xi^s = 1$. It is conventional to choose the basis $\xi^1 = \begin{pmatrix} 1 \\ 0 \end{pmatrix}$ and $\xi^2 = \begin{pmatrix} 0 \\ 1 \end{pmatrix}$, corresponding to spin up and down respectively.

The negative frequency solutions are of the form $\Psi(x) = v(p)e^{ip\cdot x}$. These are also eigenstates of H_D with eigenvalue $-E_{\mathbf{k}} < 0$ and

$$v^s(p) = \begin{pmatrix} \sqrt{p\cdot\bar{\sigma}}\,\eta^s \\ \sqrt{-p\cdot\sigma}\,(-i\eta^s) \end{pmatrix} , \tag{3.36}$$

with η^s a basis of the spin vector, normalized by $\eta^{s\dagger}\eta^s = 1$.

The field operator Ψ can now be expanded in creation and annihilation operators that obey the Fermi-Dirac anticommutation relations:

$$\Psi(x) = \int \frac{\mathrm{d}^3 p}{(2\pi)^3} \frac{1}{\sqrt{2E_{\mathbf{p}}}} \sum_s \left[a_{\mathbf{p}}^s u^s(p)e^{-ip\cdot x} + b_{\mathbf{p}}^{s\dagger} v^s(p)e^{ip\cdot x} \right] . \tag{3.37}$$

If the spin is directed along an arbitrary axis $\mathbf{n}$ then $\mathbf{n}\cdot\vec{\sigma}\,\xi = \xi$. The flipped spinor is given by $\xi^{-s} \equiv -i\sigma^2\xi^*$ because

$$(\mathbf{n}\cdot\sigma)(-i\sigma^2\xi^*) = -(-i\sigma^2\xi^*) . \tag{3.38}$$

Notice that $\xi^{-(-s)} = -\xi^s$. We associate $a_{\mathbf{p}}^s$ with the annihilation of an electron in spin state s and $b_{\mathbf{p}}^s$ with the annihilation of its antiparticle, a positron with flipped spin $-s$. So we have

$$v^s(p) = \begin{pmatrix} \sqrt{p\cdot\bar{\sigma}}\,\xi^{-s} \\ \sqrt{-p\cdot\sigma}\,(-i\xi^{-s}) \end{pmatrix} , \tag{3.39}$$

The spin direction $\mathbf{n}$ can be specified by two angles θ and ϕ. It turns out that we can write

$$\xi^1 = \begin{pmatrix} \cos(\theta/2) \\ e^{i\phi}\sin(\theta/2) \end{pmatrix} , \qquad \xi^2 = \begin{pmatrix} -e^{i\phi}\sin(\theta/2) \\ \cos(\theta/2) \end{pmatrix} .$$

The flipped spinor ξ^{-s} is given by $(\xi^{-1}, \xi^{-2}) = (\xi^2, -\xi^1)$. For completeness we state the form of the flipped annihilation operators:

$$a_{\mathbf{p}}^{-s} = (a_{\mathbf{p}}^2, -a_{\mathbf{p}}^1) \qquad \text{annihilates} \qquad u^{-s}(p) ,$$

$$b_{\mathbf{p}}^{-s} = (b_{\mathbf{p}}^2, -b_{\mathbf{p}}^1) \qquad \text{annihilates} \qquad v^{-s}(p) .$$

Now we are ready to see how the C, P, and T symmetries act. These are implemented in the same way as Lorentz transformations:

$$U(\Lambda)\Psi(x)U^{-1}(\Lambda) = \Lambda_{1/2}^{-1}\Psi(\Lambda x) . \tag{3.40}$$

Here $U(\Lambda)$ is a unitary operator acting on states, and $\Lambda_{1/2}$ is the spinor representation of Λ.

Parity Parity implies inverting the spatial momentum while keeping the spin direction fixed. The unitary parity operator $\mathcal{P}$ acts on operators as $\mathcal{P}a_{\mathbf{p}}^s\mathcal{P} = \eta_a a_{-\mathbf{p}}^s$ and $\mathcal{P}b_{\mathbf{p}}^s\mathcal{P} = \eta_b b_{-\mathbf{p}}^s$. Here η_a and η_b are possible phases that can be chosen to be $\eta_a = -\eta_b = 1$. Plugging this into equation (3.37) gives

$$\mathcal{P}\psi(t,x)\mathcal{P} = P\psi(t,-x) , \qquad \mathcal{P}\psi(\omega,k)\mathcal{P} = P\psi(\omega,-k) ,$$

$$\mathcal{P}\psi^\dagger(t,x)\mathcal{P} = \psi^\dagger(t,-x)P , \qquad \mathcal{P}\psi^\dagger(\omega,k)\mathcal{P} = \psi^\dagger(\omega,-k)P ,$$

where $P \equiv i\gamma^0$. This depends on the representation of the Clifford algebra that is used. The free Dirac Hamiltonian H_D commutes implying that the spectrum is invariant under parity. The spin operator in the z-direction is also invariant.

$$PH_D(\omega,-k)P^\dagger = H(\omega,k) .$$

$$PS^3P^\dagger = S^3$$

The Hamiltonian of the $M_1 \neq -M_2$ system does not commute because the γ^5 terms get a minus sign. This means that parity is indeed broken, as can be seen in figure (3.4). The Hamiltonian of the $M_1 = -M_2$ system does commute.

Time reversal Time reversal is an antiunitary process. Therefore it can be implemented by an antiunitary operator $\mathcal{T}$ acting on states and on complex numbers as $[\mathcal{T},a] = a^*$. Time reversal flips the spin and reverts momentum, so $\mathcal{T}a_{\mathbf{p}}^s\mathcal{T}^{-1} = a_{-\mathbf{p}}^{-s}$ and $\mathcal{T}b_{\mathbf{p}}^s\mathcal{T}^{-1} = b_{-\mathbf{p}}^{-s}$. It follows that

$$\mathcal{T}\psi(t,x)\mathcal{T}^{-1} = T\psi(-t,x) , \qquad \mathcal{T}\psi(\omega,k)\mathcal{T}^{-1} = T\psi(\omega,-k) ,$$

$$\mathcal{T}\psi^\dagger(t,x)\mathcal{T}^{-1} = \psi^\dagger(-t,x)T^\dagger , \qquad \mathcal{T}\psi^\dagger(\omega,k)\mathcal{T}^{-1} = \psi^\dagger(\omega,-k)T^\dagger ,$$

where $T \equiv -i\gamma^0\gamma^2$. The free Dirac Hamiltonian commutes so that the free theory is invariant under time reversal. The spin operator in the z-direction gets a minus sign,

$$TH_D^*(\omega,-k)T^\dagger = H_D(\omega,k) ,$$

$$T(S^3)^*T^\dagger = -S^3 .$$

The complex conjugation is due to the fact that $\mathcal{T}$ anticommutes with complex numbers. The Hamiltonian for the $M_1 \neq -M_2$ system is not Hermitian but we can write it as

$H = H_1 + iH_2$ with $H_{1,2}$ Hermitian. The Hermitian part is invariant under time reversal and the antihermitian part gets a minus sign:

$$T[H_1(\omega, -k) + iH_2(\omega, -k)]^* T^\dagger = H_1(\omega, k) - iH_2(\omega, k) = H^\dagger(\omega, k) \ . \qquad (3.41)$$

The same holds for the $M_1 = -M_2$ system.

Charge conjugation Charge conjugation interchanges particles and antiparticles while keeping the same spin orientation. It can be implemented by a unitary operator $\mathcal{C}$ acting on states. It acts on annihilation operators by conjugation, $\mathcal{C} a_{\mathbf{p}}^s \mathcal{C} = b_{\mathbf{p}}^s$ and $\mathcal{C} b_{\mathbf{p}}^s \mathcal{C} = a_{\mathbf{p}}^s$. The spinors $u^s(p)$ and $v^s(p)$ obey the following relations:

$$u^s(p) = -i\gamma^1 \gamma^3 \gamma^0 [v^s(p)]^* \ , \qquad v^s(p) = -i\gamma^1 \gamma^3 \gamma^0 [u^s(p)]^* \ .$$

Using these we can write

$$\mathcal{C}\psi(t, x)\mathcal{C} = C\psi^*(t, x) \ , \qquad \mathcal{C}\psi(\omega, k)\mathcal{C} = C\psi^*(-\omega, -k) \ ,$$

$$\mathcal{C}\psi(t, x)\mathcal{C} = C\psi^*(t, x) \ , \qquad \mathcal{C}\psi(\omega, k)\mathcal{C} = C\psi^*(-\omega, -k) \ ,$$

where $C \equiv -i\gamma^1 \gamma^3 \gamma^0$. The free Dirac Hamiltonian and the spin operator are invariant under charge conjugation,

$$C[-H_D^T(-\omega, -k)]C^\dagger = H_D(\omega, k) \ ,$$

$$C[(-S^z)^T]C^\dagger = S^z \ .$$

The minus sign comes from commuting spinor components when evaluating the expression $\mathcal{C}\psi^\dagger H_D \psi \mathcal{C}$.

In the $M_1 = -M_2$ case we have

$$C[-H^T(-\omega, -k)]C^\dagger = H^\dagger(\omega, k) \ .$$

Just as for parity the Hamiltonian for the $M_1 \neq -M_2$ case is not invariant because the γ^5 terms acquire a minus sign. This is seen in the plots by comparing figure (3.4a) with figure (3.4c) and figure (3.4b) with figure (3.4d).

CP/CPT Under the combined CP transformation we get for the $M_1 \neq -M_2$ case:

$$CP[-H^T(-\omega, -(-k))]P^\dagger C^\dagger = H^\dagger(\omega, k) \ .$$

It therefore leaves the Hermitian parts invariant. The combined CPT transformation leaves the whole Hamiltonian invariant:

$$CPT[-H^\dagger(-\omega,-k))]T^\dagger P^\dagger C^\dagger = H(\omega,k) \ .$$

From the above it is clear that the γ^5 terms in the action break parity symmetry. Since this symmetry *is* present in ultracold atom systems we must assume $M_1 = -M_2$ and thus restrict the parameter space of the bulk system. In the following chapter we will only focus on this case.

Chapter 4

The Dirac Fermion with a
Chemical Potential

In this chapter we introduce a chemical potential μ to the boundary system. This gives the massive Dirac fermions a nonzero density, which is a physical requirement when describing ultracold atom systems. This has also been done by Watse Sybesma in his master's thesis [18]. The (relativistic) dispersion relation for the non-interacting system reads

$$\omega + \mu = \sqrt{\mathbf{k}^2 + m^2} \; . \tag{4.1}$$

This means that we have to change the bulk in such a way that $\omega \to \omega + \mu$ for the free theory. The self-energy $\Sigma(\omega, \mathbf{k}, \mu)$ may depend in some nontrivial way on μ. Furthermore, a chemical potential breaks particle - antiparticle symmetry. This is seen from the fact that number of particles minus the number of antiparticles is constant. This way the chemical potential of the particles is equal to minus the chemical potential of the antiparticles.

It turns out that the way to implement the chemical potential is to charge the black brane with a charge Q_B. This is done by solving the Einsteins equations in the presence of an electric gauge potential A_μ. Since we are not interested in magnetic fields we take $A_i = 0$. To make the fermion Lagrangian gauge invariant we change the covariant derivative by

$$D_\mu \to D_\mu - i q_f A_\mu \; , \tag{4.2}$$

where q_f is a coupling constant. This process is called minimal coupling. On the boundary this results in a change

$$\omega \to \omega + \lim_{r \to \infty} q_f A_t(r) \equiv \omega + \mu \, , \tag{4.3}$$

where μ is the chemical potential. In the next section the new gravitational background will be described. This will replace the background specified in section 2.1.1, although the form will be very much the same. Only the emblackening factor V will change.

4.1 The Background of a Charged Black Brane

The metric of the charged black brane has the same form as before

$$\mathrm{d}s^2 = -\frac{V^2(r)r^{2z}}{\ell^{2z}}\mathrm{d}t^2 + \frac{\ell^2}{V^2(r)r^2}\mathrm{d}r^2 + \frac{r^2}{\ell^2}\mathrm{d}x_{d-1}^2 \, , \tag{4.4}$$

with the difference that V will now depend on Q_B, giving rise to two event horizons, just as the Reissner-Norström black hole in section 2.1.

The setup is described in [12]. Here we will give a summary of the results. To charge the black brane we have to add a $U(1)$ charge by means of an extra field $F_{2,\mu\nu} = \partial_\mu A_{2,\nu} - \partial_\nu A_{2,\mu}$, where $A_{2,i} = 0$. The background action reads

$$S_{\text{bg}} = \frac{1}{16\pi G_{d+1}} \int \mathrm{d}^{d+1}x \sqrt{-g} \left(R - 2\Lambda - \frac{1}{2}(\partial_\mu\phi)^2 - \frac{1}{4}\sum_{i=1}^{2} e^{\lambda_i\phi}F_{i,\mu\nu}F_i^{\mu\nu} \right) \, . \tag{4.5}$$

Here it looks like there are two $U(1)$ gauge fields but, as we saw before, the $F_{1,\mu\nu}$ is completely determined. The constant of motion associated with A_1^μ is related to ϕ in such a way that it provides asymptotically Lifshitz spacetime. This is the reason why the charge does not appear in the emblackening factor V. As we will see below, the constant of motion associated with A_2^μ does appear in V.

When we vary the action with respect $g_{\mu\nu}$, ϕ, and $A_{i,\mu}$ we obtain the following four equations of motion

$$R_{\mu\nu} - \frac{2\Lambda}{d-1}g_{\mu\nu} - \frac{1}{2}\partial_\mu\phi\partial_\nu\phi - \frac{1}{2}\sum_{i=1}^{2} e^{\lambda_i\phi}\left[F_{i,\mu\sigma}F_{i,\nu}^\sigma - \frac{1}{2(d-1)}F_i^2\right] \, , \, , \tag{4.6}$$

$$g^{\mu\nu}D_\mu D_\nu\phi - \frac{1}{4}\sum_{i=1}^{2} 2\lambda_i e^{\lambda_i\phi}F_i^2 = 0 \, , \, , \tag{4.7}$$

$$D_\mu\left(e^{\lambda_i\phi}F_i^{\mu\nu}\right) = 0 \, , \tag{4.8}$$

where we used in the first line

$$T_\mu{}^\mu = 0 \qquad \Rightarrow \qquad R_{\mu\nu} - \frac{1}{2}Rg_{\mu\nu} + \Lambda g_{\mu\nu} = R_{\mu\nu} - \frac{2\Lambda}{d-1}g_{\mu\nu} \ . \tag{4.9}$$

The covariant derivative D_μ contains the affine connection with the Christoffel symbols. Apart from the specific metric in equation (4.4), we assume that $A_{1,i} = A_{2,i} = 0$ and that the fields only depend on r.

The difference between the rr and tt components of equation (4.6) gives the following solution for ϕ

$$e^\phi = \alpha r^{\sqrt{2(d-1)(z-1)}} \ . \tag{4.10}$$

Here α is an integration constant, interpreted as the strength of the scalar field ϕ. Next, equation (4.8) gives us

$$F_{i,rt} = \rho_i r^{z-d} e^{-\lambda_i \phi} \ , \tag{4.11}$$

where ρ_i are integration constants. Since $\frac{\delta S}{\delta A_{i,t}} = 0$, we have two conserved currents

$$j_i^\mu = -\frac{1}{16\pi G_{d+1}} \sqrt{-g} e^{\lambda_i \phi} F_i^{t\mu} \ . \tag{4.12}$$

These give rise to two charges

$$Q_i = \int \frac{\mathrm{d}^{d-1}x}{\ell^{d-1}} j_i^0 = \frac{V_{d-1}\rho_i l^{z-1}}{16\pi G_{d+1}} \ , \tag{4.13}$$

where V_{d-1} is a dimensionless volume factor. When ρ_i is fixed, the corresponding charge is also fixed. Now, the Einsteins equations together with the equation of motion for ϕ eventually give

$$4\Lambda\sqrt{2(d-1)(z-1)} =$$
$$\sum_{i=1}^{2} \rho_i^2 r^{-2(d-1)-\lambda_i\sqrt{2(d-1)(z-1)}} \alpha^{-\lambda_i} \ell^{2(z-1)} \left[(d-1)\lambda_i - \sqrt{2(d-1)(z-1)}\right] \ . \tag{4.14}$$

This equation is solved by

$$\lambda_1 = -\sqrt{2\frac{d-1}{z-1}} \ , \quad \lambda_2 = \sqrt{2\frac{z-1}{d-1}} \ , \quad \rho_1^2 = -4\Lambda\alpha^{\lambda_1}\ell^{2(1-z)}\frac{z-1}{d+z-2} \ . \tag{4.15}$$

The cosmological constant is $\Lambda = -\frac{(d+z-1)(d+z-2)}{2\ell^2}$. The important thing to note here is that ρ_2 is still a free integration constant whereas ρ_1 is fixed in terms of the scalar field strength α. ρ_2 can be interpreted as the charge density of the black brane. It is

convenient to replace α by

$$f^2 \equiv 2(d+z-1)(z-1)\ell^{-2z}\alpha^{-\lambda_1} \ . \tag{4.16}$$

This way the solutions read

$$A'_{1,t} = fr^{d+z-2} \ , \tag{4.17}$$

$$A'_{2,t} = \rho_2 \left[\frac{1}{2(d+z-1)(z-1)} \ell^{2z} f^2 \right]^{\frac{\lambda_2}{\lambda_1}} r^{2-d-z} \ . \tag{4.18}$$

The fact that $A'_{1,t}$ diverges for $r \to \infty$ is not worrisome since it is the $A_{2,\mu}$ field that will be coupled to the fermions later. The divergence will not appear in the boundary action. The second field can be integrated such that it is zero at the horizon, $A_{2,t}(r_h) = 0$,

$$A_{2,t} = \rho_2 \left[\frac{1}{2(d+z-1)(z-1)} \ell^{2z} f^2 \right]^{\frac{\lambda_2}{\lambda_1}} \frac{1}{3-d-z} \left(r^{3-d-z} - r_h^{3-d-z} \right) \ . \tag{4.19}$$

Using equations (4.13) and (4.3) we can write the chemical potential and the electromagnetic potential as

$$\mu = q_f \frac{16\pi \bar{r}_h^{3-d-z}}{V_{d-1}(d+z-3)} Q_2 G_{d+1} \ell^{2-d} \left[\frac{f^2 \ell^{2(d+z-1)}}{2(d+z-1)(z-1)} \right]^{\frac{\lambda_2}{\lambda_1}} \ , \tag{4.20}$$

$$A_{2,t} = \frac{\mu}{q_f} \left[1 - \left(\frac{\bar{r}_h}{\bar{r}} \right)^{d+z-3} \right] \ , \tag{4.21}$$

where $r_h = \bar{r}_h \ell$. The emblackening factor is found from the Einstein equations and reads

$$\begin{aligned}
V^2(r) &= 1 - \left(\frac{r_m}{r} \right)^{d+z-1} + \rho_2 \left[\frac{\ell^{2z} f^2}{2(d+z-1)(z-1)} \right]^{\frac{\lambda_2}{\lambda_1}} \frac{\ell^{2z} r^{-2(d+z-2)}}{2(d+z-3)(z-1)} \\
&= 1 - \left(\frac{\bar{r}_m}{\bar{r}} \right)^{d+z-1} + \frac{(16\pi)^2}{V_{d-1}^2 2(d+z-3)(d-1)} \left[\frac{f^2 \ell^{2(d+z-1)}}{2(d+z-1)(z-1)} \right]^{\frac{\lambda_2}{\lambda_1}} \\
&\quad \times Q_2^2 G_{d+1}^2 \ell^{2(2-d)} \bar{r}^{-2(d+z-2)} \ ,
\end{aligned} \tag{4.22}$$

where $r = \ell \bar{r}$ and $r_m = \ell \bar{r}_m$. The quantity r_m can be expressed in terms of r_h by requiring $V(r_h) = 0$. In the next section we will identify the correct units such that the electric potential, the emblackening factor, and the chemical potential simplify and depend on clear physical quantities that can easily be translated in SI units.

4.2 Units

4.2.1 Natural Units

The background action is written in natural units, meaning $[\hbar] = [c] = 1$. This way can we express the dimensions of all quantities in terms of the length scale ℓ, that has dimension meter,

$$\underbrace{S_{\text{bg}}}_{1} = \underbrace{\frac{1}{16\pi G_{d+1}}}_{\text{m}^{1-d}} \int \underbrace{\text{d}^{d+1}x}_{\text{m}^{d+1}} \underbrace{\sqrt{-g}}_{1} \underbrace{\left(R - 2\Lambda - \frac{1}{2}(\partial_\mu \phi)^2 - \frac{1}{4}\sum_{i=1}^{2} e^{\lambda_i \phi} F_{i,\mu\nu} F_i^{\mu\nu} \right)}_{\text{m}^{-2}} . \qquad (4.23)$$

The dimensions of ρ_i, Q_i, and f are found using equations (4.11), (4.10), and (4.13) respectively:

$$[\rho_i] = \text{m}^{d-z-1} \qquad [Q_i] = \text{m}^{-1} \qquad [f] = \text{m}^{1-d-z} . \qquad (4.24)$$

From equation (4.4) it follows that the coupling constant q_f has dimension $[q_f] = \text{m}^{-1}$. The dimension of the chemical potential is energy, which in natural units becomes $[\mu] = \text{m}^{-1}$. With the above we can identify the dimensions in equation (4.20) as follows:

$$\underbrace{\mu}_{\text{m}^{-1}} = \underbrace{\bar{q}_f \ell^{-1}}_{\text{m}^{-1}} \underbrace{\frac{16\pi \bar{r}_h^{3-d-z}}{V_{d-1}(d+z-3)}}_{1} \underbrace{\bar{Q}_2}_{1} \underbrace{G_{d+1}\ell^{1-d}}_{1} \underbrace{\left[\frac{f^2 \ell^{2(d+z-1)}}{2(d+z-1)(z-1)} \right]^{\frac{\lambda_2}{\lambda_1}}}_{1} , \qquad (4.25)$$

where we defined the dimensionless charges $\bar{q}_f = \ell q_f$ and $\bar{Q}_2 = \ell Q_2$. The dimensions of the emblackening factor are given by

$$\underbrace{V^2(r)}_{1} = \underbrace{1 - \left(\frac{\bar{r}_m}{\bar{r}} \right)^{d+z-1}}_{1} + \underbrace{\frac{(16\pi)^2}{V_{d-1}^2 2(d+z-3)(d-1)}}_{1} \underbrace{\left[\frac{f^2 \ell^{2(d+z-1)}}{2(d+z-1)(z-1)} \right]^{\frac{\lambda_2}{\lambda_1}}}_{1}$$

$$\times \underbrace{\bar{Q}_2^2}_{1} \underbrace{G_{d+1}^2 \ell^{2(1-d)}}_{1} \bar{r}^{-2(d+z-2)} . \qquad (4.26)$$

Now we can perform a rescaling of $\bar{q}_f$ and $\bar{Q}_2$ such that the above two equations simplify drastically. The dimensionless rescaled charges $\hat{q}_f$ and $\hat{Q}_2$ are defined by

$$\hat{q}_f = \bar{q}_f \left[\frac{f^2 \ell^{2(d+z-1)}}{2(d+z-1)(z-1)} \right]^{\frac{\lambda_2}{2\lambda_1}} \sqrt{\frac{2(d-1)}{d+z-3}} \ , \tag{4.27}$$

$$\hat{Q}_2 = \bar{Q}_2 \left[\frac{f^2 \ell^{2(d+z-1)}}{2(d+z-1)(z-1)} \right]^{\frac{\lambda_2}{2\lambda_1}} \frac{16\pi}{V_{d-1}\sqrt{2(d+z-3)(d-1)}} G_{d+1} \ell^{1-d} \ . \tag{4.28}$$

With this the chemical potential and emblackening factor simplify to

$$\mu = \frac{1}{\ell} \hat{q}_f \hat{Q}_2 \bar{r}_h^{-(d+z-3)} \ , \tag{4.29}$$

$$V^2(r) = 1 - \left(\frac{\bar{r}_m}{\bar{r}} \right)^{d+z-1} + \hat{Q}_2^2 \bar{r}^{-2(d+z-2)} \ , \tag{4.30}$$

where $\bar{r}_m^{d+z-1} = \bar{r}_h^{d+z-1} \left(1 + \hat{Q}_2^2 \bar{r}_h^{2(2-d-z)} \right)$. The covariant derivative in the fermion action changes by

$$D_\mu \ \rightarrow \ D_\mu - \delta_\mu^0 \ i\mu \left[1 - \left(\frac{\bar{r}_h}{\bar{r}} \right)^{d+z-3} \right] \ . \tag{4.31}$$

When we restore ℓ in equation (2.16) we see that T has dimension $[T] = \mathrm{m}^{-1}$:

$$T = \frac{\bar{r}_h^{z+1}}{4\pi} \frac{\partial V^2}{\partial r} |_{r=r_h} = \frac{1}{\ell} \frac{\bar{r}_h^z}{4\pi} \left[(d+z-1) - (d+z-3)\hat{Q}_2^2 \bar{r}_h^{-2(d+z-2)} \right] \ . \tag{4.32}$$

This is of course still in natural units $[\hbar] = [c] = [k_B] = 1$. In the next part the above quantities will be expressed in SI units.

4.2.2 SI Units

Now let us comment on Poisson's law in $d+1$ dimensions and in SI units. It is valid in any dimension and has the form

$$\nabla^2 \phi_{\mathrm{grav}} = 4\pi G_{d+1}^{\mathrm{SI}} \rho_{\mathrm{mass}} \ , \qquad \nabla^2 \phi_{\mathrm{EM}} = -\frac{\rho_{\mathrm{el}}}{\epsilon_{0,d+1}} \ . \tag{4.33}$$

Here ϕ_{grav} and ϕ_{EM} are the gravitational and electromagnetic potentials respectively. The dimensions are as follows

$$[\phi_{\mathrm{grav}}] = \mathrm{J \ Kg}^{-1} \quad [\phi_{\mathrm{EM}}] = \mathrm{J \ C}^{-1} \quad [\rho_{\mathrm{mass}}] = \mathrm{Kg \ m}^d \tag{4.34}$$

$$[\rho_{\mathrm{el}}] = \mathrm{C \ m}^d \quad [\nabla^2] = \mathrm{m}^{-2} \ . \tag{4.35}$$

From this we can deduce the dimensions of G^{SI}_{d+1} and $\epsilon_{0,d+1}$,

$$\left[G^{\mathrm{SI}}_{d+1}\right] = \mathrm{m}^{d+2}\mathrm{s}^{-4}\mathrm{J}^{-1} \qquad \left[\epsilon_{0,d+1}\right] = \mathrm{m}^{2-d}\mathrm{C}^{2}\mathrm{J}^{-1} . \tag{4.36}$$

The fields $A_{i,\mu}$ are interpreted as electromagnetic potentials, of which only $A_{2,\mu}$ is physical. This motivates us to write the full background action in SI units as

$$S^{\mathrm{SI}}_{\mathrm{bg}} = \frac{c^3}{16\pi G^{\mathrm{SI}}_{d+1}} \int \mathrm{d}^{d+1}x\sqrt{-g}\left(R - 2\Lambda - \frac{1}{2}(\partial_\mu\phi)^2\right) \tag{4.37}$$

$$- \frac{1}{4\mu_{0,d+1}c} \int \mathrm{d}^{d+1}x\sqrt{-g}\sum_{i=1}^{2} e^{\lambda_i\phi}F^{\mathrm{SI}}_{i,\mu\nu}F^{\mathrm{SI},\mu\nu}_i .$$

Here the factors of c are determined by requiring $\left[S^{\mathrm{SI}}\right] = [\hbar] = \mathrm{Js}$ and using the dimensions of the integrands,

$$[R] = [\Lambda] = \mathrm{m}^{-2} \qquad [\phi] = 1 \qquad \left[F^{\mathrm{SI}}_{i,\mu\nu}\right] = \mathrm{J\ s\ C}^{-1}\mathrm{m}^{-2} . \tag{4.38}$$

The action we started with was written in natural units $[\hbar] = [c] = 1$:

$$S_{\mathrm{bg}} = \frac{1}{16\pi G_{d+1}} \int \mathrm{d}^{d+1}x\sqrt{-g}\left(R - 2\Lambda - \frac{1}{2}(\partial_\mu\phi)^2 - \frac{1}{4}\sum_{i=1}^{2} e^{\lambda_i\phi}F_{i,\mu\nu}F^{\mu\nu}_i\right) . \tag{4.39}$$

From this we deduce

$$S^{\mathrm{SI}}_{\mathrm{bg}}/\hbar = S_{\mathrm{bg}} \quad \Rightarrow \quad \frac{c^3}{\hbar G^{\mathrm{SI}}_{d+1}} = \frac{1}{G_{d+1}} , \qquad \sqrt{\frac{16\pi G^{\mathrm{SI}}_{d+1}}{c^4\mu_{0,d+1}}}F^{\mathrm{SI}}_{i,\mu\nu} = F_{i,\mu\nu} . \tag{4.40}$$

The correct form of the covariant derivative is now $D_t - i\frac{c}{\hbar}q^{\mathrm{SI}}_f A^{\mathrm{SI}}_t$, and the chemical potential is $\mu = cq^{\mathrm{SI}}_f A^{\mathrm{SI}}_t(\infty)$. Since we will use $\frac{\hbar c}{\ell}$ as our unit of energy, we can rescale q^{SI}_f such that

$$q^{\mathrm{SI}}_f\, c\, \sqrt{\frac{c^4\mu_{0,d+1}}{16\pi G^{\mathrm{SI}}_{d+1}}} = \hat{q}_f\frac{\hbar c}{\ell} . \tag{4.41}$$

Using this we obtain the following expressions for the various quantities we need when building the fermion model:

$$V^2 = 1 - \left(\frac{\bar{r}_m}{\bar{r}}\right)^{d+z-1} + \hat{Q}_2^2 \bar{r}^{2(2-d-z)} \ , \tag{4.42}$$

$$\bar{r}_m^{d+z-1} = \bar{r}_h^{d+z-1}\left[1 + \hat{Q}_2^2 \bar{r}_h^{2(2-d-z)}\right] \ , \tag{4.43}$$

$$\mu^{\mathrm{SI}} = \frac{\hbar c}{\ell}\hat{Q}_2 \hat{q}_f \bar{r}_h^{3-d-z} \ , \tag{4.44}$$

$$T^{\mathrm{SI}} = \frac{\hbar c}{k_B \ell}\frac{\bar{r}_h^z}{4\pi}\left[(d+z-1) - (d+z-3)\hat{Q}_2^2 \bar{r}_h^{-2(d+z-2)}\right] \ , \tag{4.45}$$

$$D_t \ \rightarrow \ D_t - i\frac{\mu^{\mathrm{SI}}}{\hbar}\left[1 - \left(\frac{\bar{r}}{\bar{r}_h}\right)^{3-d-z}\right] \ . \tag{4.46}$$

The free parameters of the bulk theory are $\hat{q}_f$, $\hat{Q}_2$ and $\bar{r}_h$. Now that it is clear how the rescalings work and how to switch to SI units, it is safe to work in natural units again, and derive the self-energy on the boundary.

4.3   The Spectral Function

The derivation of the spectral function is the same as in the previous chapter, with only two differences; the emblackening factor is replaced by equation (4.42) and the covariant derivative in equations (3.1) and (3.3) is replaced by equation (4.46). Since we focus on the $M_1 = -M_2 \equiv M$ case, it follows from equation (3.14) that $\xi_1(r, \omega, k_3, M_1) = \xi_2(r, \omega, k_3, -M_2) \equiv \xi(r, \omega, k_3, M)$. This means that the self-energy is fully determined by the differential equation for ξ_+, like in equation (2.66). However, because the covariant derivative is changed, this differential equation is also changed. The derivation is exactly the same and the result reads

$$r^2 V \partial_r \xi_\pm + 2Mr\xi_\pm = -\tilde{\omega} \mp k_3 + (-\tilde{\omega} \pm k_3)\xi_\pm^2 \ , \tag{4.47}$$

$$\text{where} \quad \tilde{\omega} = -\frac{\omega + \mu\left[1 - (r/r_h)^{3-d-z}\right]}{r^{z-1}V} \ .$$

Later in section 5.2 we will analyze this equation in more detail. Because the covariant derivative also appears in the kinetic term that we add by hand, the free part of the Green's function will change by $\omega \ \rightarrow \ \omega + \mu$. The Green's function, that is the analog of equation (3.31) with no γ^5 terms, reads

$$G_R(\omega, \mathbf{k}) = -\frac{(\omega + \mu - \Sigma_0)\mathbb{1}_4 + (|\mathbf{k}|^{z-1}k_i + \Sigma_i)\gamma^i\gamma^0 - im\gamma^0}{(\omega + \mu - \Sigma_0)^2 - (|\mathbf{k}|^{z-1}k_i + \Sigma_i)^2 - m^2} \ , \tag{4.48}$$

with the self-energy given by

$$\Sigma_0 = -g \lim_{r \to \infty} r^{2M} \frac{\xi_+(\omega, k_3) + \xi_+(\omega, -k_3)}{2} \ , \quad \Sigma_3 = -g \lim_{r \to \infty} r^{2M} \frac{\xi_+(\omega, k_3) - \xi_+(\omega, -k_3)}{2} \ .$$

This Green's function has two distinct two-fold degenerate eigenvalues corresponding to spin up and down particles $G_{R,+}$, and spin up and down antiparticles $G_{R,-}$:

$$G_{R\pm}(\omega, \mathbf{k}) = -\frac{1}{(\omega + \mu - \Sigma_0) \mp \sqrt{(|\mathbf{k}|^{z-1}k_i + \Sigma_i)^2 + m^2}} \ . \tag{4.49}$$

Taking the trace of G_R yields the spectral function

$$\rho(\omega, \mathbf{k}) = -\frac{1}{\pi} \text{Im} \left[\frac{\omega + \mu - \Sigma_0}{(\omega + \mu - \Sigma_0)^2 - (|\mathbf{k}|^{z-1}k_i + \Sigma_i)^2 - m^2} \right] \ . \tag{4.50}$$

The model that we have built now has a kinetic term, a finite temperature, a mass and a chemical potential. They are all ingredients of an ultracold atom system. In figure (4.1) some plots are shown of the spectral function. It is clear that the chemical potential breaks particle hole symmetry. It shifts bands, and has a nontrivial effect in the self-energy. In the next chapter we will elaborate more on this.
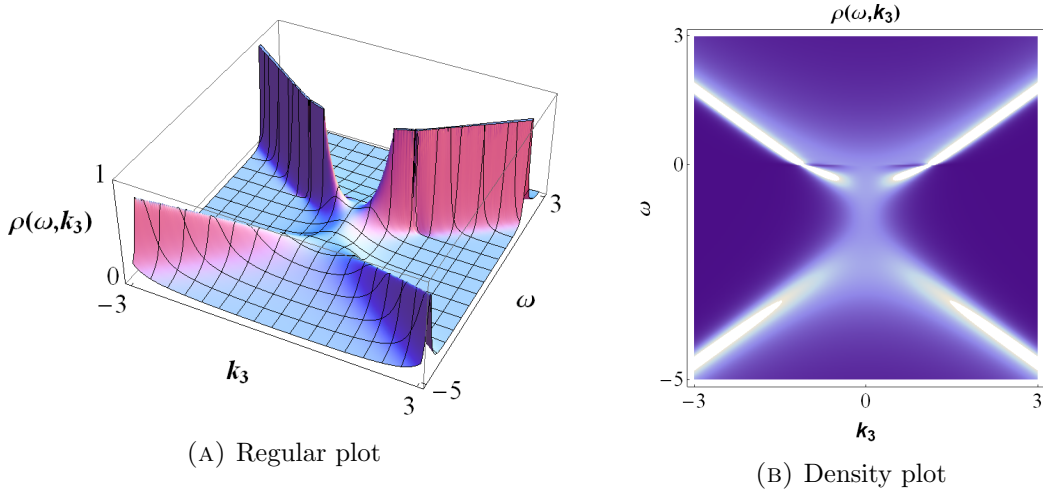

(A) Regular plot

(B) Density plot

FIGURE 4.1: Plotted is the spectral function of the massive dirac fermion, including a chemical potential. It is clear that the bands get shifted down and particle-hole symmetry gets broken. Furthermore there seems to happen something at $\omega = 0$. We will comment on this in section 5.3. The following parameters are used: $M = T = 0$, $r_h = m = z = g = 1$ and $\mu = \sqrt{2}$

Chapter 5

Properties of the Dirac Fermion

In this chapter we discuss the nonrelativistic limit of the Green's function (4.49). After that we will analyze the differential equation for ξ_+ in more detail and comment on the possible existence of multiple Fermi surfaces. In this chapter we will restrict ourselves to the $z = 1$ case.

5.1 The Nonrelativistic Limit

Before we take the nonrelativistic limit, it is useful to write the Green's function in SI units:

$$G_{R\pm}^{\mathrm{SI}}(\omega, \mathbf{k}) = -\frac{1}{\left(\hbar\omega + \mu^{\mathrm{SI}} - \frac{\hbar c}{\ell}\Sigma_0\right) \mp \sqrt{\left(\hbar c k_i + \frac{\hbar c}{\ell}\Sigma_i\right)^2 + m^2 c^4}} \ . \tag{5.1}$$

Here the self-energy Σ_μ is dimensionless because in the definitions under equation (4.48) g is dimensionless and r is replaced by $\bar{r}$. The differential equation (4.47) for ξ_+ is given by

$$\bar{r}^2 V \partial_{\bar{r}} \xi_\pm + 2M\bar{r}\xi_\pm = -\tilde{\omega} \mp \ell k_3 + (-\tilde{\omega} \pm \ell k_3)\xi_\pm^2 \ , \tag{5.2}$$

$$\text{where} \quad \tilde{\omega} = -\frac{\ell}{\hbar c}\frac{\hbar\omega + \mu^{\mathrm{SI}}\left[1 - (\bar{r}/\bar{r}_h)^{3-d-z}\right]}{\bar{r}^{z-1}V} \ ,$$

and M is a dimensionless constant. The nonrelativistic regime is characterized by

$$\hbar c |k_i| \ll mc^2 \ .$$

The square root can be expanded as

$$\sqrt{(\hbar c k_i + \frac{\hbar c}{\ell}\Sigma_i)^2 + m^2 c^4} \;=\; mc^2 + \frac{\hbar^2(k_i + \frac{1}{\ell}\Sigma_i)^2}{2m} + \mathcal{O}(1/c^2) \;. \tag{5.3}$$

Here we used that Σ_3 is defined to be antisymmetric in k_3, implying that for small enough k_3, $\Sigma_3 \sim k_3$. This results in the following nonrelativistic Green's function:

$$G_{R\pm}^{\mathrm{NR,SI}}(\omega, \mathbf{k}) = -\frac{1}{\hbar\omega + \mu^{\mathrm{SI}} - \frac{\hbar c}{\ell}\Sigma_0 \mp mc^2 \mp \hbar^2(k_i + \ell^{-1}\Sigma_i)^2/(2m)} \;. \tag{5.4}$$

The nonrelativistic chemical potential $\mu^{\mathrm{NR,SI}}$ and nonrelativistic self-energy Σ^{NR} are defined by

$$\mu^{\mathrm{NR,SI}} \equiv \mu^{\mathrm{SI}} - mc^2 - \frac{\hbar c}{\ell}\mathrm{Re}\left[\Sigma_0(0,0,\mu^{\mathrm{SI}})\right] \;, \quad \Sigma^{NR} \equiv \Sigma_0 - \mathrm{Re}[\Sigma_0(0,0)] + \frac{\hbar\Sigma_i^2}{2\ell mc} + \frac{\hbar k_i \Sigma^i}{mc} \;.$$

With these definitions the Green's functions of the upper and lower band can be written as

$$G_{R+}^{\mathrm{NR,SI}}(\omega, \mathbf{k}) = -\frac{1}{\hbar\omega + \mu^{\mathrm{NR,SI}} - \frac{\hbar^2 k_i^2}{2m} - \frac{\hbar c}{\ell}\Sigma^{\mathrm{NR}}(\omega, \mathbf{k})} \;, \tag{5.5}$$

$$G_{R-}^{\mathrm{NR,SI}}(\omega, \mathbf{k}) = -\frac{1}{\hbar\omega + \mu^{\mathrm{NR}} + \frac{\hbar^2 k_i^2}{2m} + \frac{\hbar c}{\ell}\Sigma^{\mathrm{NR,SI}}(\omega, \mathbf{k}) - 2mc^2 - 2\frac{\hbar c}{\ell}\left(\Sigma_0 - \mathrm{Re}\Sigma_0(0,0)\right)}$$

Now, since the nonrelativistic self-energy is defined such that $\mathrm{Re}\left[\Sigma^{NR}(0,0)\right] = 0$, the bands are shifted down. At $\mu^{\mathrm{NR}} = 0$, the maximum of $\rho(\omega, 0)$ will be at $\omega = 0$. In figure (5.1) the relativistic and nonrelativistic spectral functions are compared. Note that this approximation is only valid for $\hbar\omega \sim \frac{\hbar^2 k_i^2}{2m} \sim \mu^{\mathrm{NR}} \ll mc^2$. It must be noted that the shift we make to go from μ^{SI} to $\mu^{\mathrm{NR,SI}}$ is in a sense arbitrary. A possible way to do this right would be to identify the Fermi surface and subtract this energy.

One of the difficulties here is that mc^2 is not present in the self-energy whereas μ^{SI} is present in both the self-energy and the kinetic part. When we do the rescaling that is suggested above, we get the quantity $\mu^{\mathrm{NR,SI}} + mc^2$ in the self-energy. For an ultracold ^{6}Li atom gas we have $mc^2 \sim 10^{-9}$J and $\hbar\omega \sim k_B T \sim 10^{-29} J$. As a result we see that μ^{SI} in equation (5.2) is 20 orders of magnitude greater than $\hbar\omega$. This makes it very difficult to solve the differential equation.

(A) Nonrelativistic spectral function

(B) Relativistic spectral function

(C) Difference between relativistic and nonrelativistic spectral functions
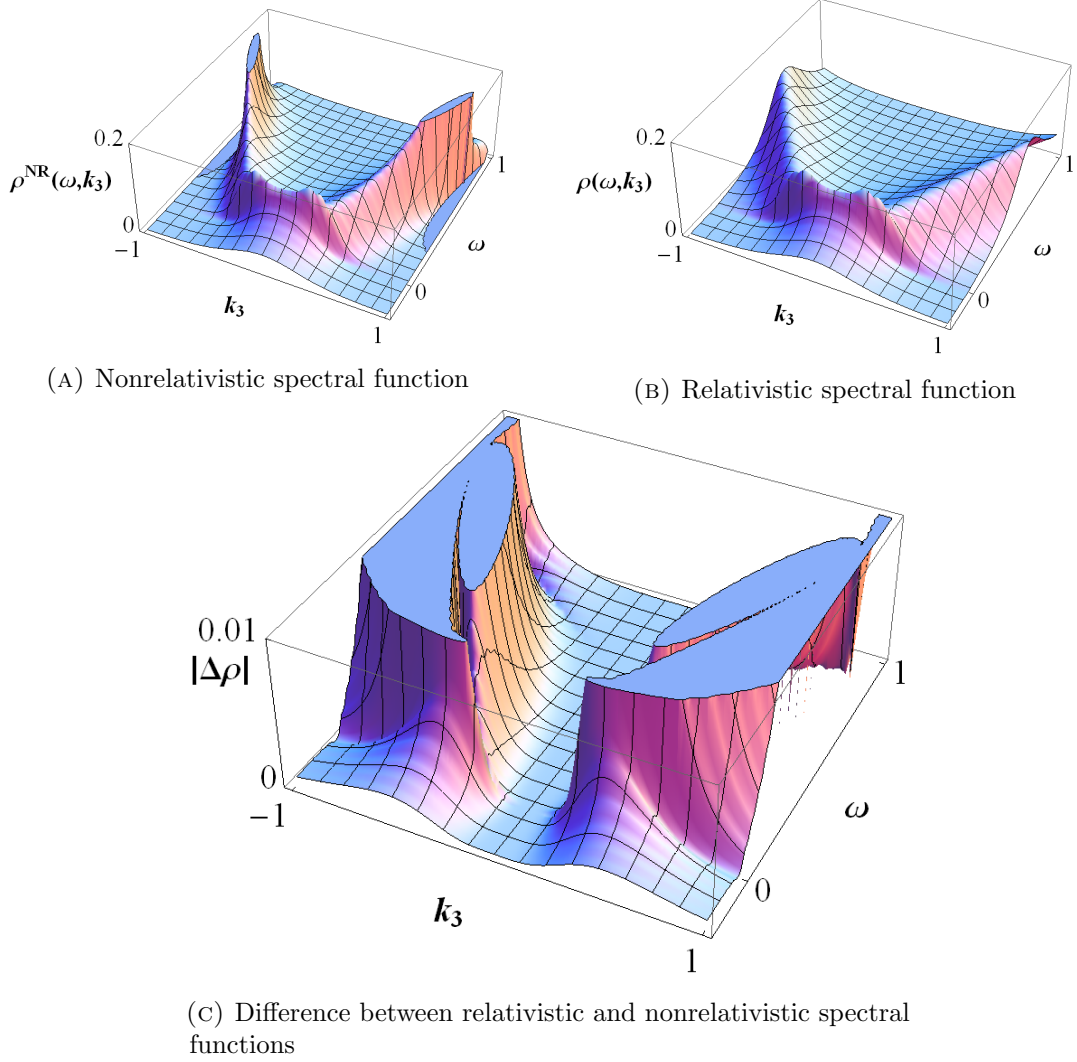
FIGURE 5.1: In the two figures on top, the spectral functions for the nonrelativistic case (5.5) and the relativistic case (4.49) are plotted. The bottom figure shows the absolute difference between the two: $\Delta\rho = \rho^{\text{NR}} - \rho$. We see that for $|k_3| < 0.1$ the approximation is valid and that it deviates for larger k_3. For large k_3 and ω we even see that ρ^{NR} becomes negative. The following parameters were used: $M = 1/4$, $T = 0$, $m = 2$, $\mu^{\text{NR}} = 0$, and $r_h = z = g = 1$.

5.2 A Closer Look at the Equation of ξ_+

In this section we will elaborate more on how to solve the differential equation for ξ_+. For simplicity we restrict the parameter space to $d = 4$, $z = 1$ and $r_h = 1$. In addition we look at zero temperature. In normal units we obtain

$$V^2 = 1 - 3r^{-4} + 2r^{-6} \ , \qquad \mu = \sqrt{2}\hat{q}_f \ , \qquad T = 0 \ . \tag{5.6}$$

The differential equation reads

$$r^2 V \partial_r \xi_+ + 2Mr\xi_+ = -(\tilde{\omega} + k_3) - (\tilde{\omega} - k_3)\xi_+^2 \ , \qquad \tilde{\omega} = -\frac{\omega + \mu[1 - r^{-2}]}{V} \ , \tag{5.7}$$

$$\lim_{\epsilon \to 0} \xi_+(1 + \epsilon) = i \ . \tag{5.8}$$

The difficulty is that $V(1) = 0$, which is the reason why we introduced the ϵ. In practice we take a small value of ϵ, solve the differential equation and check if the value was indeed small enough such that the solution converges nicely in the limit $\epsilon \to 0$. This has to be done for every (ω, k_3). The same has to be done in the limit $r \to \infty$; we must choose the cutoff value r_∞ large enough such that $r_\infty^{2M}\xi_+(\omega, k_3, r_\infty)$ is indeed close to the exact limit. Figure (5.2) gives an illustration of this method.
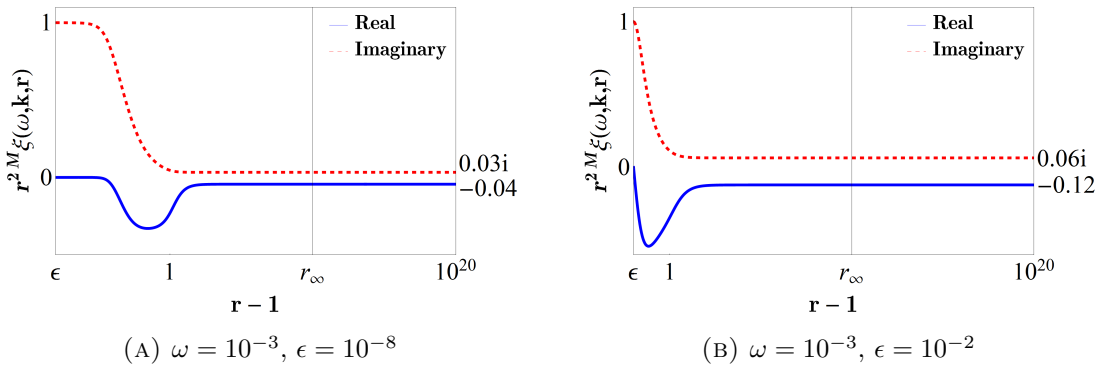

(A) $\omega = 10^{-3}$, $\epsilon = 10^{-8}$ (B) $\omega = 10^{-3}$, $\epsilon = 10^{-2}$

FIGURE 5.2: Plotted is $r^{2M}\xi(\omega, k_3, r)$ as a function of r. In the left plot the value of ϵ is small enough to make the solution converge near the horizon. In the right plot the value of ϵ is too large and the solution does not converge near the horizon. This leads to a wrong value at the boundary r_∞. In addition to the parameters defined at the beginning of this paragraph, we used $M = 0$, $m = 1$, $k = 1$, $\mu = \sqrt{2}$, $r_\infty = 10^{10}$.

It turns out that for small ω we also need small values for ϵ. For large ω the solution already converges for larger values for ϵ. This explains the apparent discontinuity at $\omega = 0$ in figure (4.1) where we took $\epsilon = 10^{-5}$. This behavior does not depend on k_3 and μ. The most straightforward way to solve this problem is to just choose a smaller value for ϵ. However this slows the numerical calculation down too much. A way around this is to Taylor expand the coefficients of the differential equation around the horizon. We

then get another differential equation that is solvable much faster, but only valid for around $r = 1$, while we need the the value at $r = r_\infty$. This is achieved by using the value of the first solution at some $r = 1 + \epsilon_2$ with $\epsilon \ll \epsilon_2 \ll 1$ as the boundary condition of the second, not Taylor expanded equation. Of course we should check that the solution is independent of ϵ *and* ϵ_2. It turns out that solving these two differential equations is faster than solving the original one with a very small value for ϵ.

The Taylor expanded differential equation whose solution is denoted by $\tilde{\xi}_+$ reads

$$\tilde{\xi}'_+ + \frac{M}{\sqrt{3}(r-1)}\tilde{\xi}_+ = \left(\frac{\omega}{12(r-1)^2} + \frac{7\omega}{36(r-1)} + \frac{\mu}{6(r-1)} \right)\left(1 + \tilde{\xi}_+^2\right)$$
$$- \frac{k_3}{2\sqrt{3}(r-1)}\left(1 - \tilde{\xi}_+^2\right) + \mathcal{O}(r-1)^0 . \qquad (5.9)$$

We expanded up to order $(r-1)^0$. Expanding further turns out to make little to no difference. The equation can be put in a nicer form by making transformation

$$e^x = (r-1) , \quad \text{such that} \quad r \to 1 \iff x \to -\infty .$$

It reads

$$\frac{\partial}{\partial x}\tilde{\xi}_+ + \frac{M}{\sqrt{3}}\tilde{\xi}_+ = \left(\frac{\omega}{12}e^{-x} + \frac{7\omega}{36} + \frac{\mu}{6}\right)\left(1 + \tilde{\xi}_+^2\right) - \frac{k_3}{2\sqrt{3}}\left(1 - \tilde{\xi}_+^2\right) . \qquad (5.10)$$

We use the value at ϵ_2 as the boundary condition of the full solution,

$$\tilde{\xi}_+(\epsilon_2) = \xi_+(\epsilon_2) .$$

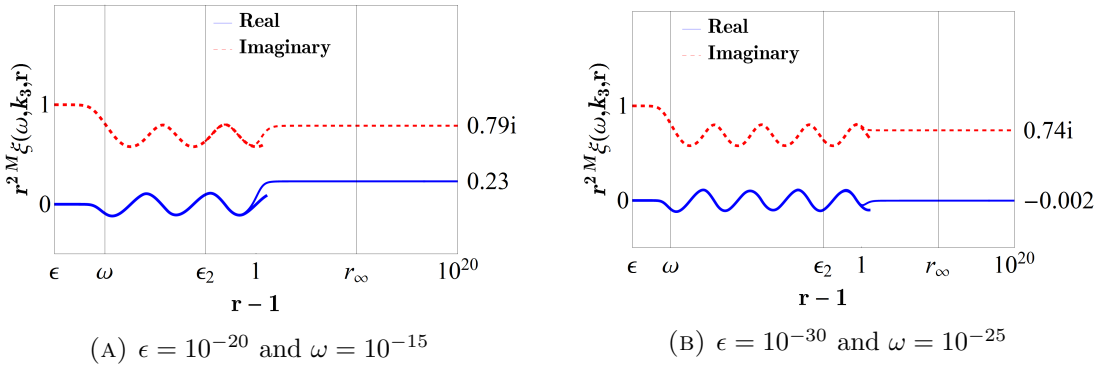The result of this procedure is shown in figure (5.3) for some generic values of the parameters.

(A) $\epsilon = 10^{-20}$ and $\omega = 10^{-15}$

(B) $\epsilon = 10^{-30}$ and $\omega = 10^{-25}$

FIGURE 5.3: Plotted is $r^{2M}\xi(\omega, k_3, r)$ as a function of r and for different values of ω and ϵ. In addition to the parameters mentioned at the beginning of this paragraph, we used $M = 0$, $m = 1$, $k_3 = 0.3$, $\mu = \sqrt{2}$, $r_\infty = 10^{10}$ and $\epsilon_2 = 10^{-5}$. From the plots it is clear that the solutions are indeed convergent on both sides, and that around ϵ_2 the Taylor expanded solution near the horizon matches the full solution.

From the above figure it is clear that for $\omega \ll r - 1 \ll \epsilon_2$ the solution exhibits oscillatory behavior and for $\epsilon \ll r - 1 \ll \omega$ convergent behavior. This is the reason why we need $\epsilon \ll \omega$, to give the solution enough space to converge. This can also be explained from equation (5.10). Note that we can neglect the $7\omega/36$ term because $\omega \ll \mu$. Now, in the region $\omega \ll r - 1 \ll \epsilon_2$ we have $\omega e^{-x} \ll \mu$, so we can also neglect this term. The solution to this equation turns out to be periodic in $x = \log(r - 1)$, and does not converge near the horizon. The convergence comes from the $\frac{\omega}{12} e^{-x}$ term, that only becomes dominant in the $\epsilon \ll r - 1 \ll \omega$ regime.

The conclusion is that we have to be careful when working with small ω because the ϵ prescription has to be adjusted accordingly. As a rule of thumb we can take ϵ to be about four orders of magnitude smaller than ω.

5.3 Signatures of Fermi surfaces

In this section we will elaborate on the properties of the spectral functions at small ω. When we zoom figure in on (4.1) a bit more we see two large peaks where the upper band crosses $\omega = 0$, see figure (5.4a). This is indicative of a Fermi surface. In fact, the same has been found by Liu, McGreevy and Vegh [4] in $d = 2 + 1$ dimensions and without a kinetic term and a mass term added to the action. Most of the properties that are discussed in this section are also found in their model.

(A) Full spectral function   (B) Logarithmic plot of the right peak.
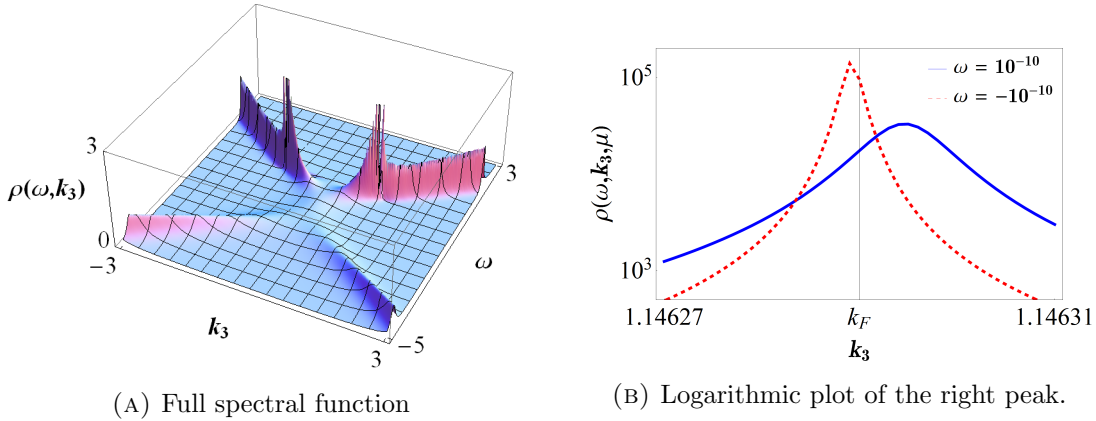
FIGURE 5.4: Plotted is the spectral function of the massive dirac fermion, including a chemical potential. The following parameters are used: $M = T = 0$, $z = r_h = m = g = 1$ and $\mu = \sqrt{2}$. In the left figure two peaks are clearly visible at $\omega = 0$ and $k = \pm k_F$. In the right figure two profiles of the peak with constant ω are given. From this we deduce that $k_F = 1.14629(5)$.

Figure (5.4b) gives a close-up view of the peak. An estimate of k_F is made by approaching $\omega = 0$ from above and below and see where the peaks meet. This peak suggests a Fermi surface with Fermi momentum k_F. The nature of the Fermi surface is characterized by the scaling of $\rho(\omega, k_F)$ as a function of ω. This is plotted figure (5.5).

(A) double logarithmic plot for $\omega < 0$
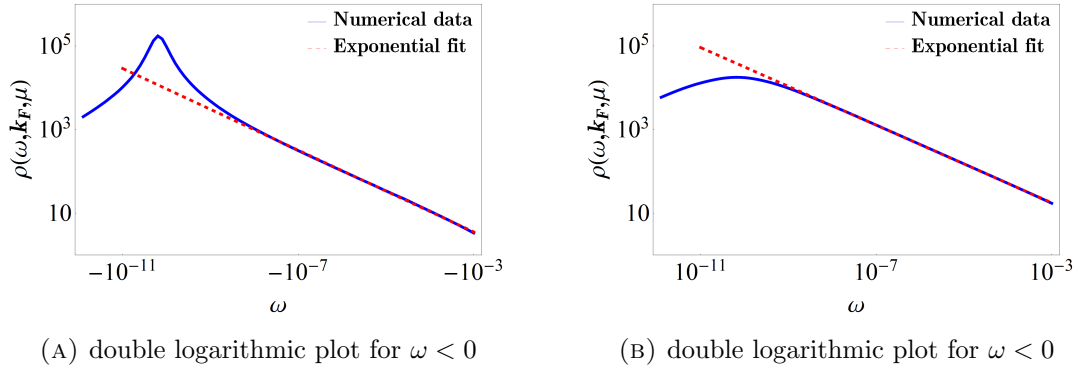

(B) double logarithmic plot for $\omega < 0$

FIGURE 5.5: Plotted is the spectral function as a function of small ω around $k \simeq k_F$. For $|\omega| > 10^{-7}$ the solution behaves as a power law to which the red/dashed curve is fitted. For $|\omega| < 10^{-7}$ we see that the solution deviates from the power law because k is not *exactly* equal to k_F. The parameters have the same values as in the previous figure.

The solution behaves as a power law for $10^{-7} \leq |\omega| < 10^{-3}$, but for $|\omega| < 10^{-7}$ it deviates from it. This is because we are not exactly at the Fermi momentum. A more precise measurement of the Fermi momentum would extend the power law to smaller ω.
The red/dashed line is the fitted power law and it reads:

$$\rho(\omega, k_F, \mu) \sim \frac{1}{|\omega|^\alpha} \ , \quad \text{with} \quad \alpha = 0.47(5) \ . \tag{5.11}$$

So the exponent is the same for either sign of ω. It must be stressed that α depends on the parameters we choose. When we take for example $m = 2$, we find $\alpha = 0.38(3)$. Now, for a conventional Landau Ferm liquid we must have $\alpha > 1$, such that there are indeed quasiparticles present. What we find now is a system that has a sharply defined Fermi surface, but no Landau quasiparticles. Such a system is called a non-Fermi liquid and has also been found in $d + 1$ dimensions [4].
The last thing that we will look at is the dependency of the spectral function on μ. It turns out that when we increase μ, more Fermi surfaces start to appear. Figure (5.6a) shows the spectral function as a function of μ and k_3 at a fixed small value of ω. Figure (5.6b) shows the spectral function as a function of ω and k_3 at a fixed μ. What we see is that for larger values of μ more bands appear. Where these bands cross the $\omega = 0$ axis, Fermi surfaces appear.

When we take $\mu = \sqrt{2}$, only one band is fully visible. the multiple band structure is only visible for higher values of μ.
This could possibly be a model for molecular states, but further study is needed to really justify such an interpretation. The scalings of the various Fermi surfaces are likely to be different and depend on the parameters of the theory. This is something that should be researched more before a clear condensed matter interpretation can be given to these results.
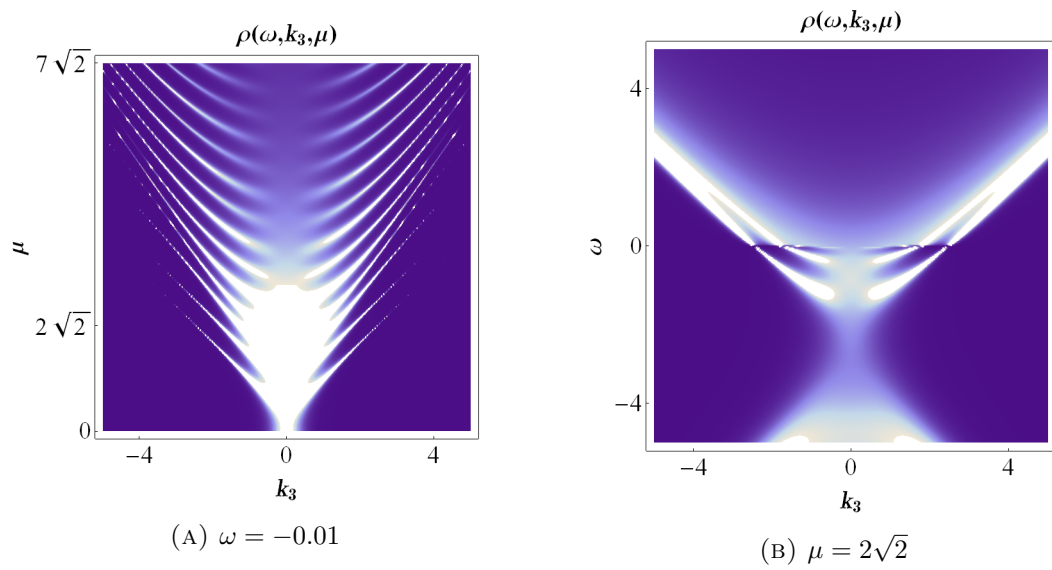
(A) $\omega = -0.01$

(B) $\mu = 2\sqrt{2}$

FIGURE 5.6: In the left figure the spectral function is plotted at fixed ω with variable k_3 and μ. In the left figure μ is fixed while k_3 and ω are varied. From the left figure it is clear that more Fermi surfaces arise with increasing μ, which translates to multiple dispersion bands in the right figure.

Chapter 6

Conclusion and Discussion

The objective of this thesis was to introduce a novel approach to condensed-matter physics by using holographic techniques. We looked at different setups with always keeping ultracold atoms in the back of our mind. The recipe that we used gave us a way to relate a classical gravity action to a single-particle Green's function.

In chapter 2 we started with the simplest model, that of a chiral fermion. The background we used is a $(d+1)$-dimensional asymptotically Lifshitz space with a black brane in the center. This background is obtained from solving Einstein's equations in the presence of some matter fields. The sole purpose of these fields is to produce the desired metric. After this we added a fermion field Ψ to the bulk, coupling it to the curved background by the covariant derivative. We neglected the backreaction of the fermion field on the metric itself. This is why the auxiliary fields that we introduced to produce the right metric do not show up in the equation of motion of Ψ. It would be interesting to see what happens when one does take backreaction into account, the equations will be much more difficult though.

After this we used the Dirac equation to integrate out the Ψ_- chiral component of Ψ and restricted the other one, Ψ_+, to the boundary. We also added a kinetic term to the action by hand. This is to get a single-particle spectral function that obeys the sum rule. The result is a spectral function of the chiral fermion consisting of a kinetic free particle part and a self-energy term.

In chapter 3 we coupled a second fermion field to the curved background and repeated the procedure of chapter 2. We got two chiral fermions on the boundary and combined them into a single Dirac spinor. Because the Dirac fermion is still massless, we added a mass term to the action by hand. The masses M_1 and M_2 of the two fermion fields in the bulk are just parameters of the self-energy on the boundary. We found that when

$M_1 \neq -M_2$, parity and charge conjugation symmetries are violated. When $M_1 = -M_2$ these symmetries do hold. Since parity symmetry is present in ultracold atom systems, we restricted ourselves to the latter case.

In chapter 4 we went one step further and added a chemical potential to the system by replacing the uncharged black brane by a charged black brane. This is done by adding a U(1) gauge field to the matter action in chapter 2. The difference with the other matter fields is that this gauge field *does* couple to the fermion fields by means of an extra term in the covariant derivative. We saw that this term takes the form of a chemical potential on the boundary. We had to carefully analyze the dimensions of all the terms and perform some rescalings, which resulted in equations (4.42)-(4.46). As expected the chemical potential breaks particle-antiparticle symmetry.

In chapter 5 we first looked at the nonrelativistic limit of the Green's function derived in chapter 4. The difficulty here was that the chemical potential μ appears in both the kinetic and self-energy terms while the mass m does not appear in the self-energy. This means that when we shift μ with a factor of mc^2, we get a huge difference in orders of magnitude in the differential equation for ξ. We did however verify that for $\hbar c |\mathbf{k}| \ll mc^2$ the nonrelativistic approximation holds, and we found an expression for the nonrelativistic self-energy. It would be interesting to investigate this further and find some way to apply it to a real physical system such as ultracold ^{6}Li atoms.

Finally we looked at signatures of Fermi surfaces. What we found were two sharp peaks in the spectral function at $\omega = 0$. This is an indication of a Fermi surface, but not of a regular Landau Fermi surface because the scaling is different, see equation (5.11). The systems that have this property are called non-Fermi liquids and they are strongly coupled. Furthermore we saw in figure (5.6) that with increasing μ there appear multiple bands and multiple Fermi surfaces. This confirms earlier results in $d = 3$ dimensions [4]. These multiple bands could possibly be interpreted as the states of a molecule. This is however very sketchy and further research is needed to confirm this claim.

In addition to this it would be interesting to know more about the influence of all the parameters in the theory. For example in figure (5.6a) we see that the position of the outermost Fermi surface shifts with increasing μ, so $k_F(\mu)$ is a function of μ. Because the width also changes, the scaling will be different too. This means that the coefficient α in equation (5.11) depends on the position of the Fermi surface: $\alpha(k_F)$. In future research it would be interesting to study this behavior more.

Another thing one could look at is the equation of state. The number density $n(\mathbf{k}, \mu)$ can be calculated by $n(\mathbf{k}, \mu) = \int_{-\infty}^{\mu} d\omega \rho(\mathbf{k}, \omega)$. Integrating this over $\mathbf{k}$ gives $N(\mu)$; the equation of state of the system.

Bibliography

[1] J. M. Maldacena. The large N limit of superconformal field theories and supergravity. *Adv. Theor. Math. Phys.*, **2**(231), 1998. [arXiv:hep-th/9711200].

[2] E. Witten. Anti de sitter space and holography. *Adv. Theor. Math. Phys.*, **2**(253), 1998. [arXiv:hep-th/9802150].

[3] S. A. Hartnoll. Lectures on holographic methods for condensed matter physics. *Classical and Quantum Gravity*, **26**(22), 2009. [arXiv:0903.3246 [hep-th]].

[4] J. McGreevy. Holographic duality with a view toward many-body physics. 2010. [arXiv:0909.0518 [hep-th]].

[5] J. Zaanen, Y. Sun, Y. Liu, and K. Schalm. The AdS/CMT manual for plumbers and electricians. 2012. [lorentz.leidenuniv.nl/ kschalm/papers/adscmtreview.pdf].

[6] B. Zwiebach. A First Course in String Theory. 2009. p.549. ISBN-13 978-0-521-88032-9.

[7] U. Gursoy, E. Plauschinn, H. Stoof, and S. Vandoren. Holography and ARPES sum-rules. *JHEP*, **1205**(018), 2012. [arXiv:1112.5074 [hep-th]].

[8] R. Contino and A. Pomarol. Holography for fermions. *JHEP*, 2004(11):058, 2004. [arXiv:hep-th/0406257].

[9] H. Stoof, K. Gubbels, and D. Dickerscheid. Ultracold Quantum Fields. 2009. ISBN: 978-1-4020-8762-2.

[10] H. Liu, J. McGreevy, and D. Vegh. Non-fermi liquids from holography. *Phys. Rev. D*, **83**:065029, 2009. [arXiv:0903.2477 [hep-th]].

[11] J. Polchinski. Effective field theory and the fermi surface. 1999. [arXiv:hep-th/9210046].

[12] J. Tarrio and S. Vandoren. Black holes and black branes in lifshitz spacetimes. *JHEP*, 1109:017, 2011. [arXiv:1105.6335 [hep-th]].

[13] N. Poplawski. Spacetime and fields. [arXiv:0911.0334 [gr-qc]].

[14] J. Laia and D. Tong. Flowing between fermionic fixed points. *JHEP*, 1111:131, 2011. [arXiv:1108.2216 [hep-th]].

[15] J. Wu W. Li. Holographic fermions in charged dilaton black branes. *Nucl. Phys. B*, 867:810–826, 2012. [arXiv:1203.0674 [hep-th]].

[16] U. Gursoy, V. Jacobs, E. Plauschinn, H. Stoof, and S. Vandoren. Holographic models for undoped weyl semimetals. *JHEP*, 4:127, 2013. [arXiv:1209.2593 [hep-th]].

[17] M. Peskin and D. Schroeder. An Introduction to Quantum Field Theory. 1995. ISBN: 0-201-50397-2.

[18] W. Sybesma. Weyl Semimetals and Holography. *Master's Thesis*, 2012. [thesis.pdf].

Acknowledgements